CHAPTER

3

Molly A. Schnirring-Judge

Utility of Nuclear Medicine Imaging in the Diabetic Foot

INTRODUCTION

Given the fact that patients with longstanding diabetes are often fraught with coincident neuropathy and an impaired immune system, they prove challenging in all facets of medical management and imaging is no exception. In the face of clinically significant neuropathy with or without autonomic dysfunction, the patient with diabetes is at high risk for occult trauma. Given this fact, it is not unusual for these patients to suffer from injury that results in infection or wound healing complications that increases their morbidity and mortality rate. When nuclear medicine imaging (NMI) is used early in the diagnostic workup, significant clinical and physiologic information can be verified. With the most commonly used techniques, important physical details can be documented, such as blood flow to an organ or limb, bone reactions such as arthropathy, contusion, or fracture, as well as the discrete white blood cell accumulations seen in infection. Although the science behind NMI is the same regardless of the patient type, it is particularly useful in patient populations that present with combinations of structural abnormalities, acute arthropathy, and infections.

HISTORICAL REVIEW

The discovery of radioactivity is attributed to Henri Becquerel in 1896. His findings inspired his assistant, Madame Curie, to pursue research and analyses of uranium and its by-products leading to the isolation of polonium and radium. The Nobel Prize for physics in this research was shared by Becquerel and Marie and Pierre Curie in 1903. In 1911, Marie Curie received a second Nobel Prize in chemistry for her work in the radioactivity associated with uranium and its decay products. Therapeutic properties were discovered from the study of radium, and this remains the basis for the host of NMI used in clinical medicine and therapeutics today.

Although the imaging technology behind nuclear medicine dates back to the early 1900s, the first scanner used for isotope imaging, the rectilinear scanner, was developed in 1951 by Benedict Cassen. In 1952, Hal Anger developed the first scintillation camera, the Anger camera, which has served as the prototype for present day camera systems. Over time, its use in musculoskeletal imaging has been researched and developed for specific categories of pathology. By the 1980s, computed tomography advanced nuclear medicine into the world of cross-sectional imaging and single photon emission computed tomography (SPECT) systems moved to the forefront of NMI. This sectional imaging technique was first used for research in cerebral and cardiac imaging, although today SPECT can be applied to all organ systems. Examples of this imaging technique are provided later in this chapter.

Although any organ system can be studied with the benefit of nuclear medicine techniques, perhaps one of its greatest strengths is in musculoskeletal imaging. Nuclear medicine imaging has facilitated the study of lower extremity neoplasms (soft tissue and bone), hypercoagulable states such as sickle-cell anemia and deep vein thrombosis, fractures, contusions, and the spectrum of arthropathy to include bone and joint infections. Nuclear medicine technology includes radiolabeled leukocyte and antibody imaging, which has become a very powerful tool for diagnosing infection and is particularly useful in imaging acute and chronic inflammatory conditions of the lower extremities. Repeating NMI after clinical cure can confirm or refute the absence of indolent or subclinical infection. Complex foot and ankle deformities such as the combination of the Charcot foot with concomitant ulceration and infection pose an arduous challenge to the surgeon and as such ancillary imaging techniques such as NMI help to shed light on these limb-threatening conditions. An academic review of the nature of this imaging modality and illustrations of common radiolabeled imaging techniques will underline the clinical utility of NMI in identifying and discriminating between the various complications of diabetes in the lower extremity, including the Charcot foot and infections of soft tissue or bone.

ACADEMIC FUNDAMENTALS

The clinical value of NMI lies in the visual data it produces. Radiolabeled compounds emit energy from radionuclide (radioisotope) decay, and that is what puts an image on the film. Much like a radiograph exposes film with electron energy, radionuclides expose film using gamma, alpha, or beta ray

emissions in the very same way. Although a radiograph produces a positive image on the film (white image on black background), a radioisotope emits energy that produce negative images (black on white). The mechanics of this can be discussed very simply. In a radiograph, a structure is placed in front of the film. The radiographs emitted shed all of their energy, exposing the film to black or they penetrate structures that absorb energy allowing less energy to expose the film. The structures that absorb energy, such as bone, muscle, and tendon, allow a smaller percentage of energy to be delivered onto the film, creating a spectrum of shades ranging from white to very dark gray. The soft tissues of muscle, tendon, fat, and skin absorb much less energy and block a smaller fraction of x-ray energy, allowing various shades of gray to be imaged on film. When a radioisotope produces an image, the energy is emitted from inside a structure, and as it leaves (the limb or organ) it loses energy and exposes the film accordingly. The trick to NMI is getting the isotope to the structure or region of interest. For this, an isotope must be linked to a chemical that will take it to the target organ or structure. A radiochemical (radiolabeled compound) is an isotope linked to a chemical; the chemical takes the isotope to the target, where the majority of the isotope's energy is imparted; hence, the term radiolabeling of a chemical. It is intuitive then that a compound that has a natural affinity to bone would be able to localize an isotope and produce images of that structure. A good example of this is the routine bone scan that uses technetium methylene diphosphonate (Tc-MDP). Methylene diphosphonate is taken up by the hydroxyapatite crystal of bone, where it becomes fixed within the crystalline structure. The isotope technetium is bound there, emitting its energy for the duration of its physiologic half-life. Different imaging protocols involve deliberate combinations of chemicals and isotopes depending on the desired target organ. Each radiochemical localizes at a predictable rate; therefore, imaging schedules vary. Since isotopes vary depending on their energy of emission and physical half-life, they are used in differing quantities to minimize radiation exposure to the patient accordingly.

BONE AND SOFT TISSUE IMAGING

From a practical perspective, musculoskeletal imaging techniques primarily use technetium. Technetium (^{99m}Tc) has a short half-life of 6 hours, and is readily available labeled to chemicals that are physiologic in nature. These compounds are essentially inert and there is virtually no incidence of allergic reaction to them, which is a great advantage over other imaging modalities that use iodine or other contrast materials. Technetium-99m is a metastable isotope; therefore, it has a short physical half-life. (The m in ^{99m}Tc indicates that the isotope is metastable and therefore decays quickly, resulting in a short physical half-life.) It emits a low-energy gamma ray emission of 140 kV that imposes a minimum of radiation exposure to the patient. These properties make technetium a readily available isotope with excellent imaging characteristics. Technetium imaging in particular is performed for the identification of arthritic changes, avascular necrosis, avulsion fractures, diseases resulting in marrow expansion of bone (e.g., sickle cell disease and intraosseous tumors), diabetic gangrene, fibrous dysplasia, reflex sympathetic dystrophy, hypertrophic osteoarthropathy (HOA), neoplasms, and metabolic abnormalities. Any region of hyperemia in soft tissue or bone will exhibit an increased area of uptake on a technetium scan. Osseous injury resulting from bone fracture (surgically induced or traumatic), hypertrophic nonunion of bone, or osteomyelitis treated to cure will continue to reveal hyperemia from continued bone remodeling for more than 1 year after the initial insult (Fig. 3.1). Therefore, a thorough history is integral to appropriate interpretation of these studies. Technetium-99m alone localizes in multiple organ systems of the body; therefore, to achieve specific target localization, the isotope is labeled to a chemical. The chemical action determines what tissue or organ system is visualized. In short, the chemical localizes the isotope in the target tissue/organ and the isotope emits the radiation energy that produces the image. Remember that these chemical compounds are distributed via the intravascular compartment and many are eliminated by the renal system (tubular filtration or glomerular filtration). For this reason, a bone scan using technetium requires increased hydration to clear background activity and improve the target-to-background ratio. To accomplish this, the patient is instructed to drink 32 oz of fluid after the injection and returns in approximately 2 hours for third phase scanning. In cases of severe peripheral vascular disease or renal vascular impairment, the delivery of the radiochemical will be delayed and may compromise the target to background ratio seen upon imaging. Figure 3.1 illustrates a healthy 38-year-old patient with normal renal vascular status. Contrast that to images seen in Figures 3.2B and 3.5B, in which diabetic patients with multisystem compromise (including chronic renal failure) increase the background radiation and reduce image resolution in third phase bone scan imaging.

The triphasic bone scan, using ^{99m}Tc-MDP, is helpful in discriminating among cellulitis, abscess, and osteomyelitis by comparing their respective imaging patterns. Cellulitis shows an increased intensity in the initial phase and then diminishes throughout the second and third phases of the study. A soft tissue abscess will reveal intense localized uptake throughout the first two phases of the study, but will wash out in the third phase if there is no bone involvement in the pathology. The third phase of a triphase scan reveals bone uptake of the isotope and facilitates the differentiation between soft tissue and bone pathology. Oblique positioning during the second and third

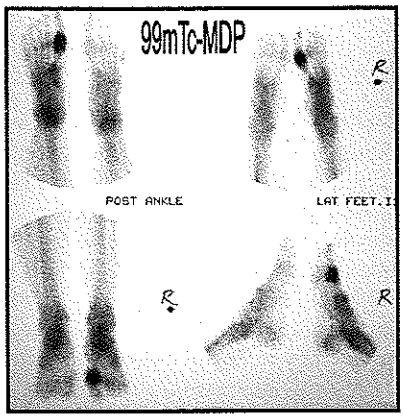

Figure 3.1 ^{99m}Tc-MDP scan demonstrates synovitis 1 year s/p first metatarsophalangeal silicone implant. Three phases confirm localized hyperemia about the implant; however, this is not enough to confirm or refute the presence of infection. Notice that the small bones of the forefoot are readily identified and can be imaged in multiple orthogonal planes to better separate bone from adjacent soft tissue structures.

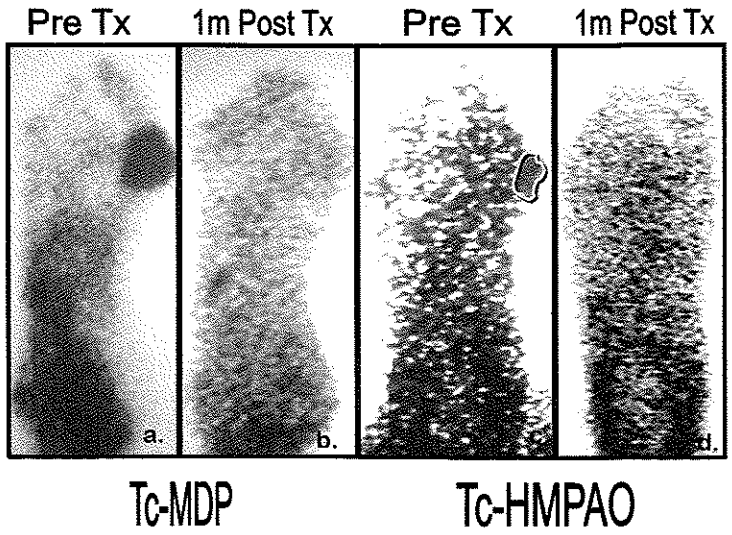

Figure 3.2 This case represents a diabetic patient with longstanding ulceration and acute onset of redness, warmth, swelling, and tenderness in a bunion deformity. The side-by-side comparison of the Tc-MDP third phase and Tc-HMPAO imaging depicts septic arthritis. **A.** A positive Tc-MDP third phase scan in the region of the first metatarsal phalangeal joint (MTPJ) shows increased activity in the region of the proximal phalanx base and the first metatarsal head before surgical débridement and antibiotic therapy. The obliquity of this view throws the first MTPJ away from that of the second MTPJ ruling out associated joint involvement. The "photogenic" character of ^{99m}Tc-MDP allows resolution sufficient to separate out the small bones of the lesser tarsus here. **B.** ^{99m}Tc-MDP after treatment confirming that there is no residual bone remodeling supporting the clinical cure of septic arthritis. **C.** ^{99m}Tc-HMPAO before surgical débridement and antibiotic therapy. The region of interest is outlined to delineate a smaller focus of activity versus that identified on the ^{99m}Tc-MDP scan suggesting only localized medial eminence involvement. This illustrates the lower target-to-background ratio of Tc-HMPAO as compared with Tc-MDP. **D.** ^{99m}Tc-HMPAO 3 weeks after completion of 4 weeks of oral antibiotic therapy. Cultures obtained before a delayed primary closure confirmed the absence of infection in the first metatarsal head.

phases is usually sufficient to provide separation of the soft tissue structures from bone delineating abscess formation that exists tangential to bone structures. In contrast, osteomyelitis shows an increased localized uptake in all three phases of imaging. It is important to note that the diagnosis of osteomyelitis cannot be made from a third phase ^{99m}Tc-MDP bone scan as it illuminates areas of hyperemia without clarifying its etiology. Definitive diagnosis of infection requires further imaging to identify an appropriate location for bone biopsy when it is warranted. Although the bone scan is sensitive for many processes associated with hyperemia, this study lacks specificity; as a consequence, it is only to be used as a screening tool.

The differentiation in appearance between osteomyelitis and septic arthritis in routine bone scanning is not commonly discussed. However, it is understood that these two conditions are distinct clinical entities and demonstrate different behavior patterns in NMI. In the face of septic arthritis, it is possible to identify the articulations involved as being separate and distinct from soft tissue structures outside or even adjacent to the joint periphery. Although the initial pattern of uptake on these images is identical to that seen in osteomyelitis, follow-up imaging patterns for these two entities are decidedly different. In the case of osteomyelitis, the affected bone will yield an increased uptake on a ^{99m}Tc-MDP scan long after clinical cure. Experience has shown that this uptake can be demonstrated a year or more after clinical cure because of ongoing remodeling of bone (MSJ). In contrast, once clinical cure has been achieved for a septic joint, long-term follow-up studies will return to baseline without third phase isotope uptake as there is no residual hyperemia in either soft tissue or bone once a septic joint is resolved (Fig. 3.2A–D).

The triphasic bone scan is also useful in studying the spectrum of bone healing. Any condition that includes remodeling of bone will produce an increased region of uptake on all three phases of the triphase scan. Injury to bone such as fracture (iatrogenic, pathologic, or traumatic), contusion, or dislocation will elicit three phases of uptake because of associated hyperemia. The ^{99m}Tc-MDP scan in particular is helpful in sorting out conditions such as delayed union and nonunion of bone and will reveal distinct patterns of uptake in cases of hypertrophic or atrophic nonunions.

INFECTION IMAGING

It is important to gain a general understanding of the physical properties of the more commonly used isotopes in nuclear medicine leukocyte imaging as they determine the imaging characteristics of each radiolabeled compound. An overview of the most commonly used isotopes in infection imaging is provided in Table 3.1. The following is an academic review of commonly used isotopes and their respective roles in infection imaging.

Nuclear medicine imaging techniques for the identification and isolation of infection have been in use since the 1950s.

TABLE 3.1 Comparison of Radioisotopes

Isotope	$T_{1/2}$	*Energy*[a]	*Dose*[b]	*Production*[c]	*Availability*
Technetium (^{99m}Tc)	6.0 hr	Gamma 140	5.0–10.0	Generator	Abundant
Indium (^{111}In)	2.8 d	Gamma 173–247	0.5–1.0	Cyclotron	Limited
Gallium (^{67}Ga)	3.25 d	Gamma 100–400	0.5	Generator	Abundant
Flourine (^{18}F)	109 min	Photon 511	10.0	Cyclotron	Limited

[a]Energy of emissions in kilo electron volts (kV).
[b]Dosages reported in millicuries of radioactivity.
[c]Method of production directly impacts isotope availability.

Gallium is one of the first isotopes used to localize infections and other pathologic processes. This agent binds with transferrin, which is an iron bound protein found within the cytoplasm of white blood cells (WBCs). An intravenous injection of gallium citrate provides an in vivo labeling of leukocytes and bacterial organisms allowing for the identification of inflammatory processes (Fig. 3.3A,B) (2). Notice from Figure 3.3 that this agent has a normal distribution within soft tissue structures of the entire body and includes delineation of glandular structures within the head and neck region. It has been primarily used in the study of fever of unknown origin and is still used today. Since the introduction of gallium imaging for infection, research has brought about the development of alternate radiolabeled WBC studies to enhance the specificity and imaging quality of these exams.

In 1976, indium-oxine-leukocyte imaging (^{111}In-oxine-WBC imaging) came to the forefront and since that time has enjoyed a large degree of clinical usage. Indium delineates leukocyte accumulation, providing a faithful mirror of WBC activity within 24 hours. Over time, this imaging technique has earned its place in the study of both acute and chronic infectious processes (3–18). Indium imaging, like gallium, suffers from inherently poor imaging characteristics, as it emits dual high-energy alpha rays to produce its images. This results in poor spatial resolution and a low target-to-background ratio. This technique often requires a minimum of 24 hours to localize within an area of WBC accumulation. Depending on the differential diagnosis, imaging may be obtained in series at 6, 24, 48, and 72 hours. In cases of positive uptake, the region of isotope localization becomes more discrete as time progresses because of the combined effect of the physical and biologic half-life of the compound. Improved localization occurs over time as a result of lowered background radiation and an improvement in target-to-background ratio. At the time this was the best imaging agent available for the noninvasive investigation of infection. Indium leukocyte imaging has remained a primary imaging agent for the localization of infectious processes despite its poor imaging characteristics and low spatial resolution (Fig. 3.4).

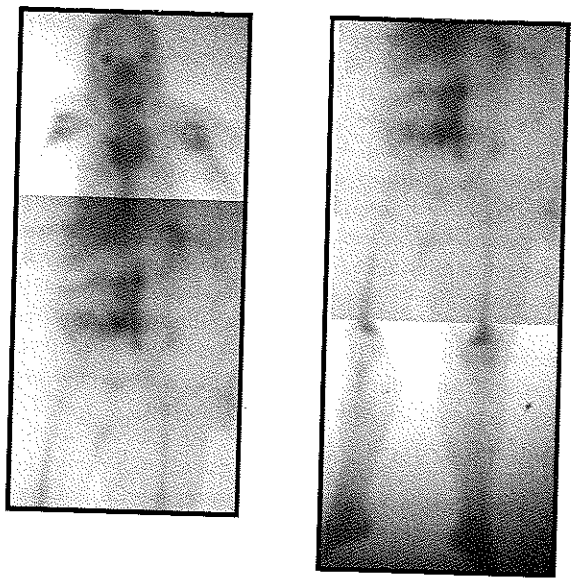

Figure 3.3 Total body image of a gallium citrate scan for ruling out occult infection. Notice that this is primarily a soft tissue imaging agent with normal areas of uptake, including the lacrimal and salivary glands. It is commonly used in the search for occult infection in cases of fever of unknown origin. Gallium can isolate and differentiate among a spectrum of pathologies, including inflammatory bowel disease, cyst, and abscess and tumor formation.

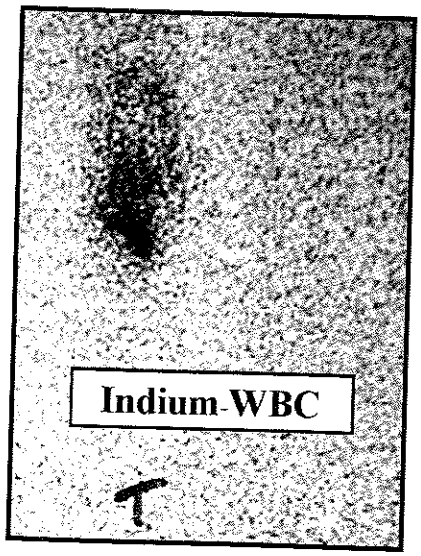

Figure 3.4 Positive indium leukocyte studies appear very grainy, with localized white cell accumulation demonstrated as clusters of small, black, often pinpoint regions of intensity. In this image the "T" indicates the direction of the toes, and the reader's right and left correspond to the medial and lateral aspect of the foot, respectively. Notice that there is no anatomic information to specifically identify the location of the leukocyte accumulation in this image, which is an inherent pitfall of the indium-leukocyte technique.

In the late 1980s interest would be rejuvenated in NMI as a new and improved radiolabeled white cell technique came to the forefront. In 1986 technetium −99m-d,l hexamethyl propylene amine oxime aka Tc-HMPAO (CERETEC) would be developed for cerebral perfusion imaging using the isotope technetium, hence the trade name CERETEC. The excellent imaging characteristics of the isotope ^{99m}Tc enhanced nuclear medicine tomography in cerebral imaging immensely. Since HMPAO has a high affinity and avidity in labeling to WBCs, it was later suggested for imaging in cases of infection. Technetium is a very "photogenic" isotope because of its low energy of emission and short half-life. That is to say, technetium has favorable imaging characteristics providing improved spatial resolution in imaging that is not achievable using either indium or gallium. By combining technetium with HMPAO, the resulting compound has both high affinity and avidity to leukocytes (because of the HMPAO) and produces images with improved structural resolution (because of the technetium) (Fig. 3.5C). Improvement in spatial resolution is best appreciated when compared directly with other infection imaging agents such as gallium citrate and indium-oxine-leukocyte compounds. The benefit of improved imaging resolution using technetium increased the specificity of radiolabeled WBC imaging and therefore improved the technique. Tc-HMPAO imaging has proved to have great utility in some of the most complicated and challenging of infectious conditions (19–47). This includes both the evaluation and management of postoperative infection and differentiating osteomyelitis from adjacent soft tissue infection (1). Like indium-leukocyte imaging, phlebotomy is required and a physical labeling of WBCs is performed in vitro. This compound is then reinjected into the patient and imaging with ^{99m}Tc-HMPAO- leukocytes is generally performed at 6, 18, and 24 hours after injection, which may vary with the institution performing the study. This technique is used for the evaluation of clinical conditions suspicious for infection and the management of postoperative infection, and for differentiating osteomyelitis from adjacent soft tissue infection. Although a bone scan in the third phase is helpful in identifying regions of hyperemia, the HMPAO study elucidates well-localized areas of white cell accumulation or infection and can be very helpful when determining discrete sights for bone débridement or bone biopsy procurement (Fig 3.5A,B). It is important to understand that a diagnosis of osteomyelitis cannot be made from a routine bone scan using any NMI agent. Definitive diagnosis of osteomyelitis requires the gold standard of bone biopsy.

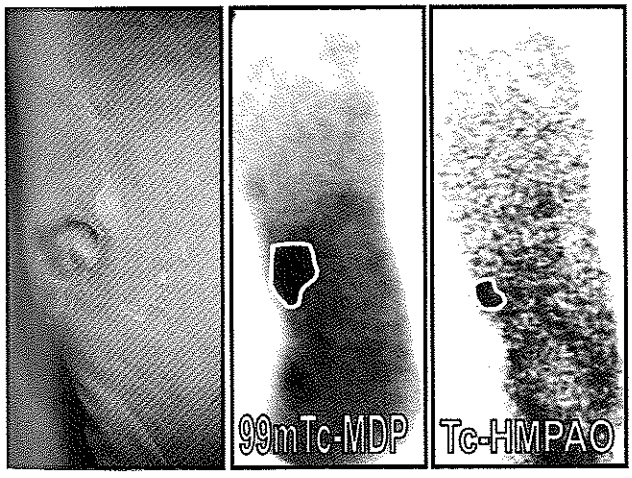

Figure 3.5 The third phase of a bone scan is helpful in identifying regions of hyperemia. In this diabetic patient **(A)** suffering from chronic renal failure (CRF), it is easy to appreciate a large region of increased radiotracer uptake in the region of the fourth and fifth metatarsal bases and distal cuboid **(B)**. Given the presence of CRF the target-to-background ratio is poor, resulting in a loss of contrast between the soft tissues and bone. **(C).** In this ^{99m}Tc-HMPAO leukocyte image there is a well-localized focus of radiotracer activity that best defines the extent of infection. This serves as a useful guide in determining the site for bone débridement and biopsy.

The current literature suggests using ^{99m}Tc- sulfur colloid as an imaging alternative for the diagnosis of osteomyelitis (7,15). Sulfur colloid is an albumin of sufficient particle size to permeate the reticuloendothelial system (RES), which includes the liver, spleen, and bone marrow. When combined with the isotope ^{99m}Tc, the colloid can localize within the RES organs and illuminate the target of interest. ^{99m}Tc-sulfur colloid deposition in bone marrow provides information about the intraosseous compartment by identifying space-occupying lesions, as it is truly a marrow-imaging agent. The colloid will not permeate a nidus of infection, malignancy or other neoplastic entity rather it delineates the pathology as a dead space or void, resulting in an area of photopenia (lack of isotope uptake). In the author's experience using this technique in the lower extremity, the small bones of the tarsus have been poorly demonstrated. It is likely that larger bones with a greater cubic content of marrow will be more easily visualized using this technique (Fig. 3.6D). This image illustrates the lack of structural detail and failure to delineate skeletal contours when using ^{99m}Tc-sulfur colloid in the small bones of the foot and ankle. This case underscores the complexity of diabetic foot ulceration in an amputee. Despite the fact that a transmetatarsal amputation was performed 1 year ago, the region of bone resections remain intense on the ^{99m}Tc-MDP bone scan. Even in the absence of infection, these regions should exhibit intensity on the routine bone scan because of continued bone remodeling, but the question remains as to whether there is an infection associated with the bone underlying a region of nonhealing ulceration. One can consider MRI in this event; however, there are likely to be postsurgical changes in bone and soft tissue changes because of active ulceration that confound its interpretation (Fig. 3.6A–E). Hypertrophic bone formation shows local radiotracer uptake the same as any other remodeling bone, which is well illustrated in Figure 3.6B,C.

All imaging techniques used for the identification of infection are judged based on their respective sensitivity and specificity. Depending on the author and the research protocol used, these data vary dramatically for NMI in the current literature (48). Many argue that magnetic resonance imaging (MRI) is the best modality for the diagnostic challenge of identifying osteomyelitis as it will predictably show a decreased signal in T1 images and increased signal on T2 images in the face of a degenerative inflammatory process in bone (49–57). The sensitivity and specificity of MRI for infection is commonly reported as 94% to 100% and 69% to 96%, respectively. Unfortunately, other conditions that distort normal anatomy will confound the reading of an MRI; such as the case of postsurgical changes or the coincidence of Charcot neuroarthropathy and infection

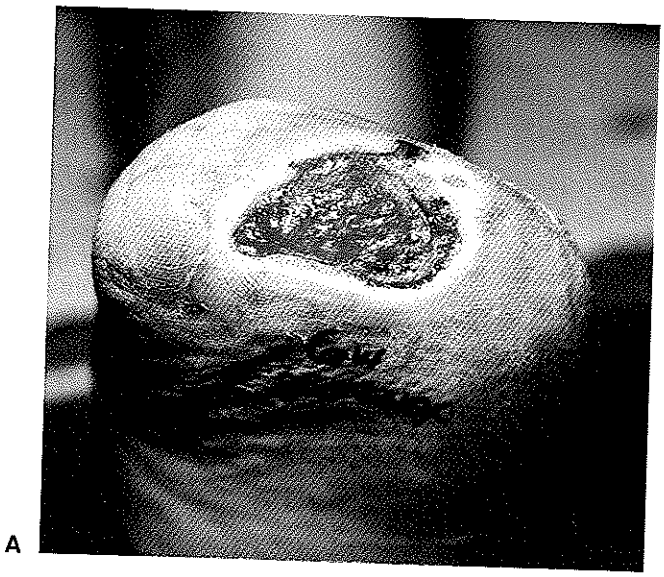

A

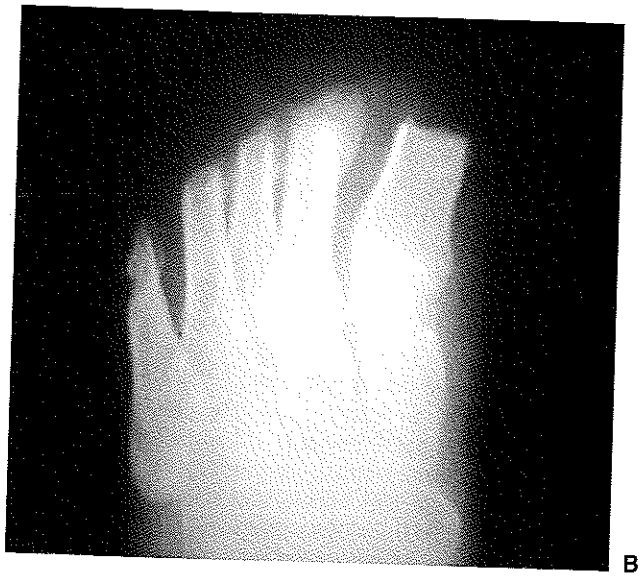

B

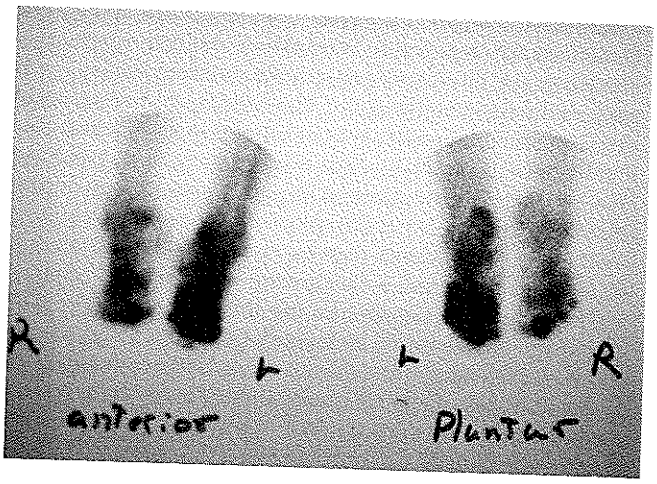

C

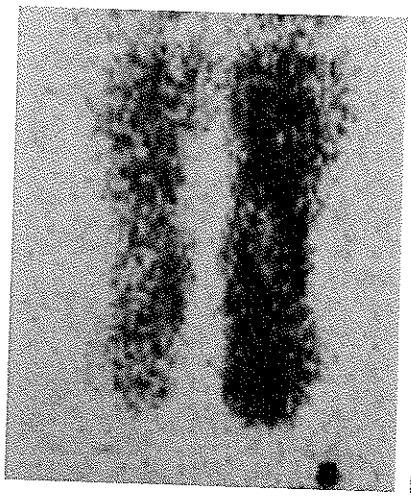

D

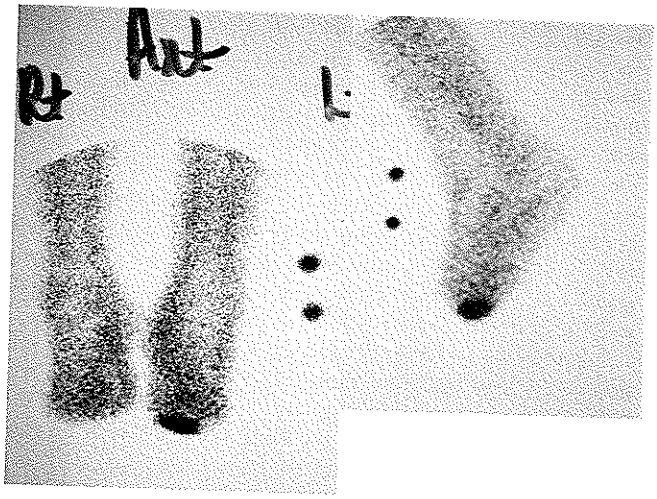

E

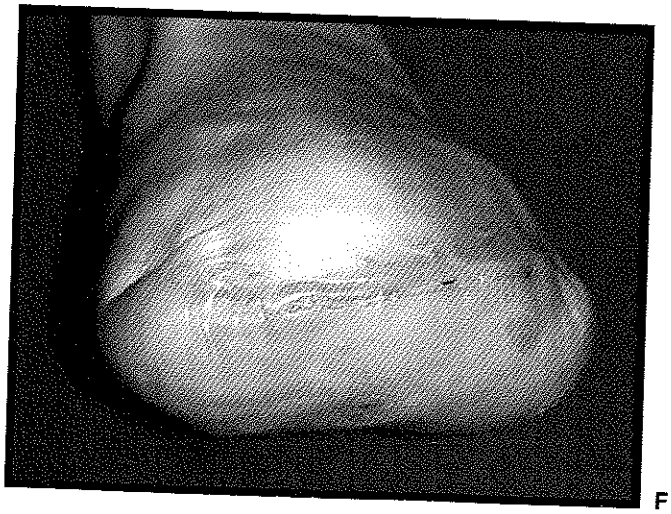

F

Figure 3.6 **A.** Clinical photo 1 year post–left transmetatarsal amputation. Ulceration develops in the distal stump and is persistent despite 6 weeks of local wound care and offloading. **B.** The left DP radiograph reveals evidence of hypertrophic bone formation about the lesser metatarsal stumps as well as penciling of the fifth metatarsal. **C.** The third phase bone scan in the presence of a well-healed transmetatarsal amputation continues to show evidence of bone remodeling even at 1 year after surgery. This study is interpreted as suggestive of infection and clinical correlation is suggested. **D.** This marrow scan using ^{99m}Tc-sulfur colloid illustrates a lack of structural detail and failure to delineate skeletal contours in foot and ankle imaging. Sulfur colloid fails to provide meaningful structural detail given the small cubic content of the marrow cavities in residual metatarsal shafts. **E.** The indium leukocyte study reveals accumulation of radiotracer within the distal soft tissue structures without evidence of discrete bone infection. **F.** Surgical débridement and bone recontouring is required to achieve healing. This clinical photo is taken 8 months postoperatively.

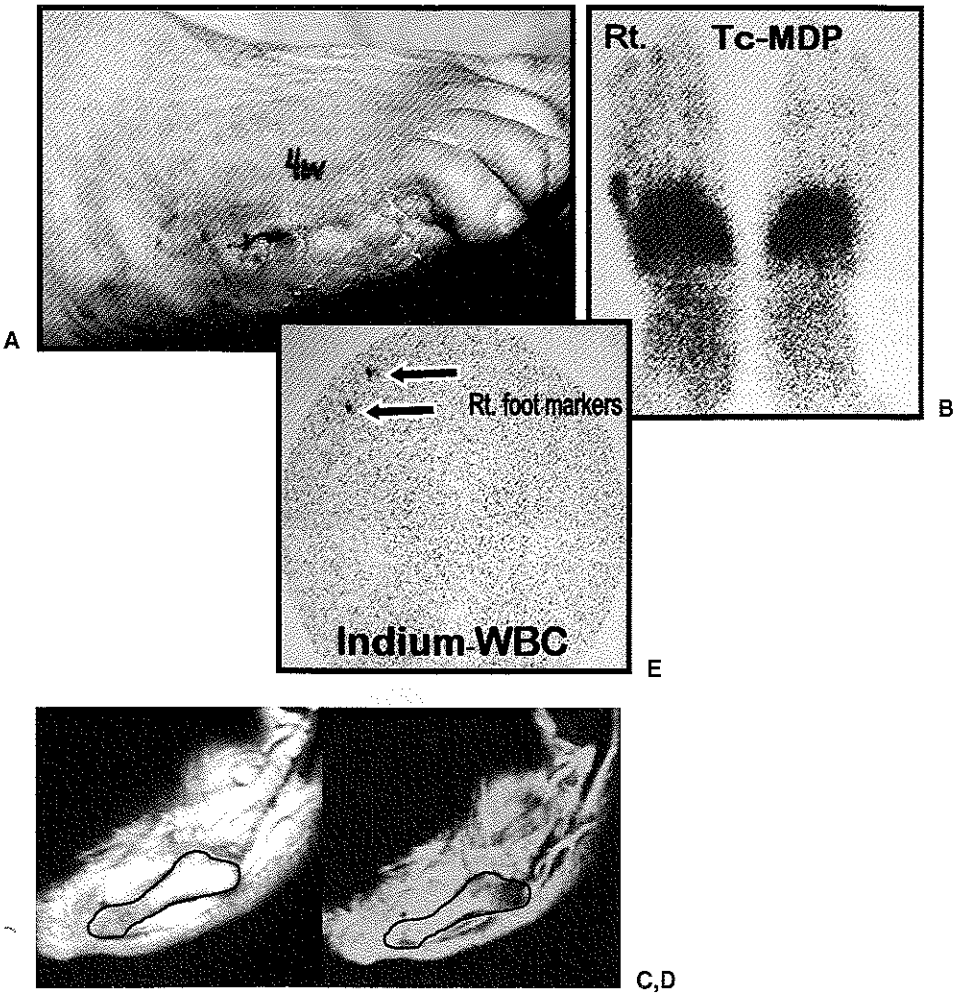

Figure 3.7 **A.** Nonhealing wound just 4 weeks after fifth digit amputation and biopsy of fifth metatarsal head was confirmed negative for osteomyelitis by both microbiology and histology. Emergency room referral for an MRI was interpreted as strongly suggestive of osteomyelitis across the entire mid foot warranting amputation. As the patient is known to have a burned out Charcot process, the case became complicated regarding the extent of potential infection and coincidence of infection. **B.** The ^{99m}Tc-MDP bone scan reveals hyperemia in the fifth ray because of postsurgical change as well as hyperemia of a burned out Charcot process across the Lisfranc joint. **C.** MRI revealing decreased signal intensity within the distal one third of the fifth metatarsal on T1 imaging. **D.** MRI revealing increased signal within the majority of the fifth metatarsal segment, indicating that the inflammatory process invades the majority of this long bone. **E.** There is *no* localized accumulation of indium leukocytes anywhere in the foot or ankle. The diagnosis is then confirmed as a chronic ulceration without evidence of soft tissue or bone infection, resulting in limb salvage.

(Fig. 3.7A,B). It is extremely important to note that, in its active state, Charcot neuroarthropathy will show a very similar MRI pattern to osteomyelitis. The mixed lytic and resorptive destruction that occurs in bone because of infection is indistinguishable from the destruction that is seen in actively progressive neuropathic disease demonstrated on MRI (11,49,50,58). Differentiating between Charcot joint and infection is among the most important diagnostic challenges in lower extremity pathology and NMI is often a helpful tool in discerning the two conditions as separate and distinct (Fig. 3.7B,E).

COMBINATION IMAGING TECHNIQUES (^{111}IN-WBC/^{99M}TC-MDP)

When an ^{111}indium-oxine-WBC study identifies a focus of infection, it becomes apparent that there is no structural detail to these images. As seen in Figure 3.4, an accumulation of WBCs is easily appreciated; however, the specific location of the accumulation cannot be determined using this image alone. The combination of an indium-WBC image and a routine bone scan (^{99m}Tc-MDP) provides more specific identification of leukocyte accumulation. The combination imaging technique uses the structural information provided by ^{99m}Tc-MDP for plotting out regions of leukocyte accumulation as identified by the ^{111}In-oxine-WBC scan (1,11,12–15,48,59–62) (Fig. 3.8A–D). An overlay or side-to-side comparison of these studies optimizes interpretation of the data set. In general, the ^{99m}Tc MDP bone scan, specifically the third phase bone image, is used to provide structural information that allows mapping of the precise location of WBC accumulation when compared with an ^{111}In-oxine-WBC scan. It is felt that correlation in two or more orthogonal planes is important when attempting to differentiate infectious processes that occur in or adjacent to areas of sterile inflammation as occurs in active arthropathy or acute neuropathic disease states (10). Using grid markings, it is possible to express the location of isotope uptake via X-Y coordinates. By using the same field of view without moving the patient, the technetium and indium images are obtained and the anatomic landmarks can be cross-correlated for comparison. This outline of the foot makes it easy to compare foot positioning between these two studies. Multiple orthogonal planes of imaging are helpful in clarifying the localization of infection when it exists. To obtain markings and orthogonal views such as these, specific communications between the ordering physician and nuclear medicine technologist are required and in the author's (MSJ) opinion are well worth the additional effort.

Combination imaging to differentiate soft tissue infection from osteomyelitis has been repeatedly suggested in the liter-

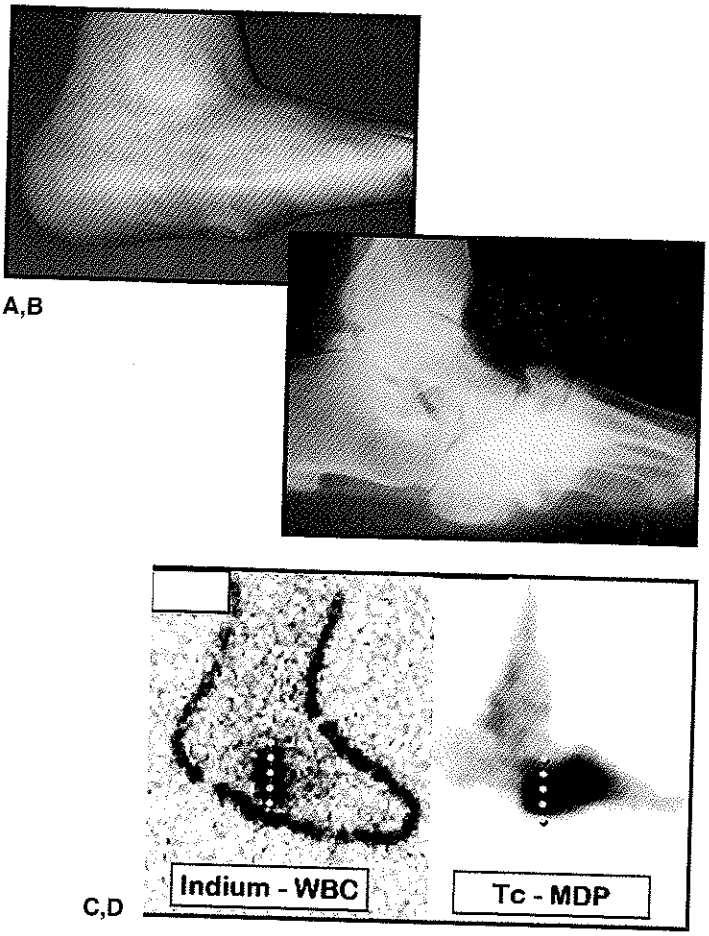

Figure 3.8 This illustrates the combination imaging technique using ^{99m}Tc-MDP and indium-WBC. **A.** This clinical photo demonstrates an area of ulceration with localized erythema, warmth, and edema 3 years after an acute Charcot breakdown. **B.** This lateral radiograph shows the end result of neuropathic breakdown; a rocker bottom foot with a plantar flexed cuboid bone creating a pressure point and ulceration. **C.** This ^{99m}Tc-MDP study illustrates the study's high sensitivity for areas of hyperemia as is seen in a Charcot foot. Hyperemia suggests an inflammatory and or infectious process exists; therefore, this study alone does not reconcile the issue of Charcot versus osteomyelitis. **D.** This indium leukocyte study has the outline of the extremity drawn on the image using the indium syringe. This outline of the foot makes it easy to compare foot positioning between these two studies. To obtain markings such as these, specific communications between the ordering physician and the nuclear medicine technologist are required. The combination of indium leukocyte imaging and ^{99m}Tc-MDP delineates the region of an infectious process within the cuboid bone while at the same time ruling out the existence of infection elsewhere within the degenerated Chopart joint. Using a grid coordinate system, seen here as a large dotted line, discrete areas of infection on the indium scan can be cross-correlated with the anatomic outline on the MDP scan in preparing for bone biopsy and débridement.

ature to enhance the specificity and sensitivity of nuclear medicine leukocyte studies. The overall sensitivity and specificity of NMI has been reported ranging from 75% to 100% and 70% to 100%, respectively (11,15,48,63). These statistics vary from author to author as their protocols often compare numerous nuclear medicine techniques of differing sensitivities and specificities.

INTERPRETATION OF RADIONUCLIDE LEUKOCYTE IMAGING

The interpretation of NMI studies is chiefly the responsibility of the radiologist; however, the ordering physician should have a good working knowledge of the goals of the study and how images are to be interpreted and clinically correlated. This should include a thorough understanding of conditions that are associated with an increased leukocyte accumulation and those that are not. With this understanding, the clinician can better predict when a false-positive or -negative result is possible. This allows better prognostication for the patient and an improved clinical approach to the pathology.

Specific recommendations regarding how to interpret the combination of ^{99m}Tc-MDP and ^{111}In-oxine or ^{99m}Tc leukocyte images include grading the intensity of uptake, congruence of intensity, and congruence of the size of the region of leukocyte uptake in comparison with that of the unaffected contralateral limb. Combination imaging allows for cross-comparison that further delineates the specific location of pathology and pro-

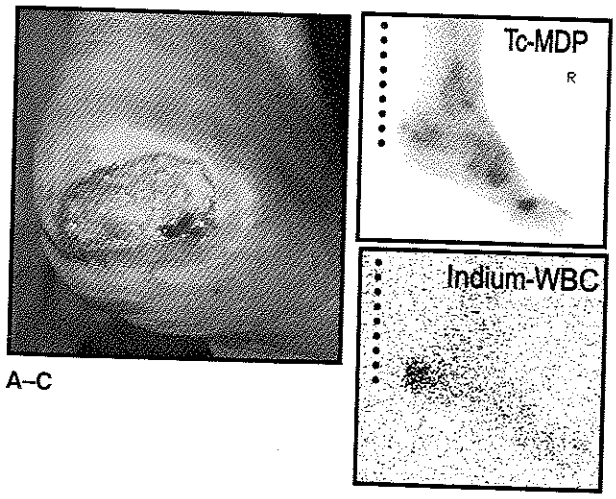

Figure 3.9 **A.** Clinical photo of a recurrent right posterior heel decubitus in the face of diabetes and end stage peripheral vascular disease. The longstanding nature of this wound, periodic over 1.25 year, prompts the investigation for underlying osteomyelitis. **B.** Third phase Tc-MDP fails to identify localized radionuclide uptake in the heel bone. **C.** Combination imaging here is effective in identifying soft tissue infection using ^{111}-Indium-WBC. These images identify leukocyte accumulation in the posterior aspect of the heel consistent with soft tissue infection and support the pursuit of soft tissue débridement. A core biopsy of the posterior heel is guided by the findings in this image and fails to identify organisms of infection or histiologic change in bone suggestive of infection.

vides skeletal mapping of white cell accumulation that is helpful in preparing for bone biopsy procurement (Fig. 3.8C,D) (8,11,15,62).

To appropriately interpret radiolabeled leukocyte studies, it is important to understand disease states other than infection that prompt leukocyte accumulation to predict when a false-positive image may result. Alternately, understanding those conditions that do not prompt leukocyte accumulation will help to further narrow the differential diagnosis in the face of a negative leukocyte scan. The radionuclide leukocyte study will remain negative in the presence of severe degenerative arthritis, migratory polyarthritis, metastatic bone disease, and aseptic necrosis. A mild increased uptake has been reported in the presence of closed fracture, delayed or nonunion of bone, and total joint implant arthroplasty (9,10). Clinical conditions that may prompt sterile inflammatory reactions may result in false-positive studies including heterotopic bone formation, myositis ossificans, and fulminant rheumatoid arthritis or active neuropathic disease.

NUCLEAR MEDICINE IMAGING IN NEUROPATHIC JOINT DISEASE: THE CHARCOT FOOT

INTRODUCTION

The diagnosis of neuropathic joint disease is reliant on a combination of radiographic and clinical findings. The earliest reports of neuroarthropathy, also known as Charcot joint, consisted of isolated case reports and small group studies with little or no long-term follow-up. These reports were of little value in attempting to study the natural history of progression of this condition and consequently did not aid in prognostication. Over time, increasing awareness of the link between some systemic diseases and neuroarthropathy has paved the way for research and follow-up of patients demonstrating signs of neuropathic joint disease and dysfunction. When complex conditions ensue and a combination of lower extremity infection, ulceration, acute edema, and/or neuropathic joint disease develop, especially in diabetic patients, there should be a high degree of suspicion for an impending Charcot foot.

One of the largest retrospective reviews of Charcot foot to date identified this condition as being associated with a host of systemic diseases with or without associated neuropathy. The epidemiologic data of 101 patients in that study describes patients within their fifth and sixth decades of life with longstanding insulin-dependent diabetes mellitus (>15 year duration) affecting men and women with essentially the same prevalence. Nearly one third of these patients suffered with triopathy—the combination of peripheral neuropathy, nephropathy, and retinopathy—a combination of pathologies that increase the incidence of occult trauma and impaired wound healing capacity. In this series of patients the tarsometatarsal joint, metatarsophalangeal joints, and ankle were affected in descending order of prevalence with >20% demonstrating bilateral disease (64). Typically, patients present because of structural deformity, whereas ulcerations and joint swelling are among the alternate presenting complaints. Bone prominences may exist in any anatomic plane; however, dorsal and plantar prominences with or without keratoses and rocker bottom foot types seem to be discussed most commonly in the literature. It is when these clinical scenarios are compounded by erythema, edema, and calor with or without deep pain that merits a more detailed examination, as they may well be complicated by infection. The presence of an open ulceration further complicates the clinical presentation. In obtaining a definitive diagnosis, the first priority is to eliminate that diagnosis associated with the highest degree of morbidity, while in the interim developing a treatment strategy to ensure that further arthropathy is prevented; that is, the part is immobilized.

In the face of active Charcot neuroarthropathy, an increased area of uptake in the 4-hour ^{111}indium-oxine-WBC image will correlate with plain radiographic changes consistent with the acute Charcot flare (11). A subsequent "washout" phenomenon has been identified in these patients occurring between the 4- and 24-hour images that Schauwecker described (Fig. 3.10) (58). In the absence of infection, this abnormal uptake and subsequent washout phenomenon in active neuroarthropathy is presumably because of the development of hematopoietically active bone marrow that accompanies active Charcot arthropathy (15,48). This active marrow is thought to be the result of the fracture repair process that accompanies the destructive changes and remodeling typified in the Charcot joint. The conversion of fatty marrow to hematopoietically active marrow may be because of increased cytokine activity. When there is a concomitant area of infection, the washout phenomenon is not seen and an area of persistent increased intensity delineates the focus of white cell activity and infection in delayed imaging. This is a scintigraphic finding that helps differentiate active Charcot neuroarthropathy from osteomyelitis (58). The washout phenomenon can be subtle and is important to discern when planning for a bone biopsy procedure. Understanding this phenomenon is integral to an accurate interpretation of

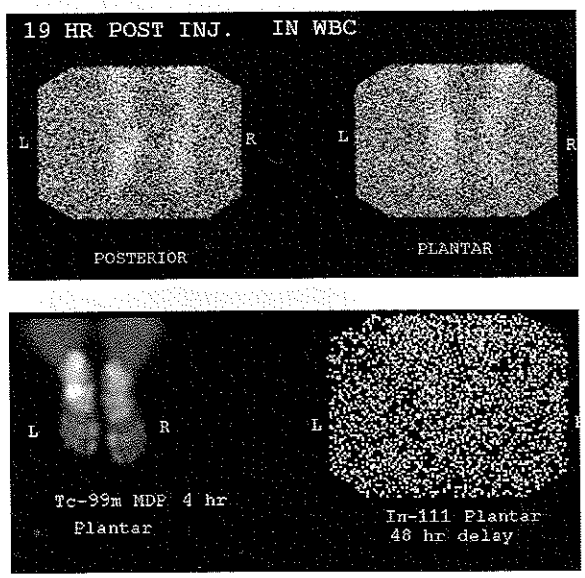

Figure 3.10 **A.** An indium scan fails to elucidate any evidence of localized leukocyte accumulation. However, there is a generalized increase in intensity throughout the left limb with neuropathic fracture. **B.** This illustrates side by side the increased intensity of the cuboid bone fracture on the Tc-MDP scan with the complete washout of activity at 24 hours in the indium scan. This is felt to corroborate Schauwecker's findings regarding acute phase uptake of neuropathic bone followed by washout in the 24 hour scan.

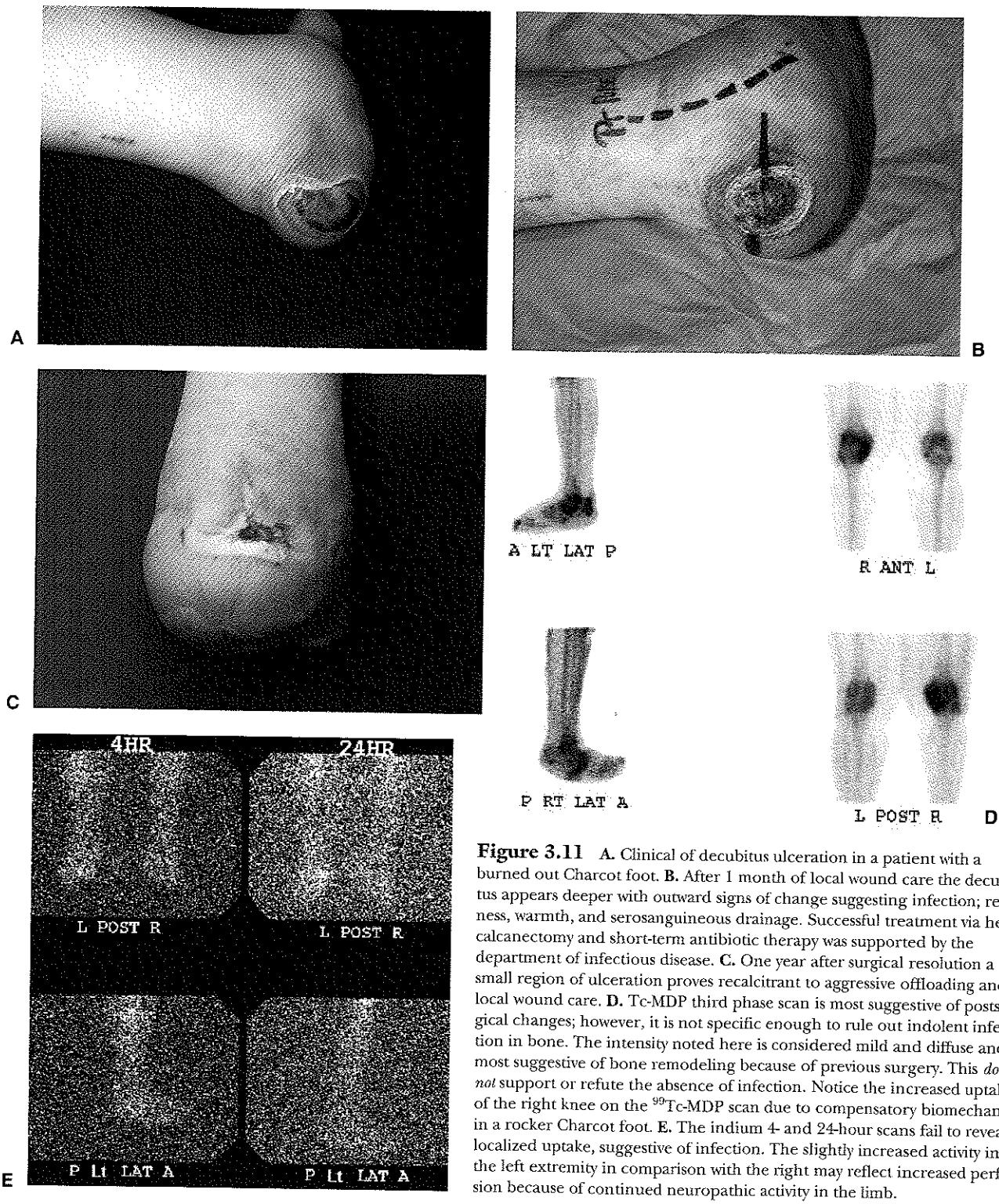

Figure 3.11 **A.** Clinical of decubitus ulceration in a patient with a burned out Charcot foot. **B.** After 1 month of local wound care the decubitus appears deeper with outward signs of change suggesting infection; redness, warmth, and serosanguineous drainage. Successful treatment via hemicalcanectomy and short-term antibiotic therapy was supported by the department of infectious disease. **C.** One year after surgical resolution a small region of ulceration proves recalcitrant to aggressive offloading and local wound care. **D.** Tc-MDP third phase scan is most suggestive of postsurgical changes; however, it is not specific enough to rule out indolent infection in bone. The intensity noted here is considered mild and diffuse and is most suggestive of bone remodeling because of previous surgery. This *does not* support or refute the absence of infection. Notice the increased uptake of the right knee on the ^{99}Tc-MDP scan due to compensatory biomechanics in a rocker Charcot foot. **E.** The indium 4- and 24-hour scans fail to reveal localized uptake, suggestive of infection. The slightly increased activity in the left extremity in comparison with the right may reflect increased perfusion because of continued neuropathic activity in the limb.

leukocyte imaging in clinical conditions that involve Charcot neuroarthropathy and the risk of coincident infection. In the face of a "burned out" Charcot arthropathy affected joints are expected to have an increased area of intensity on ^{99m}Tc-MDP bone scan but do not prompt leukocyte accumulation on the NMI exam (Figs. 3.7B,E and 3.11D,E). In the case of active Charcot neuroarthropathy and coincident infection, when it exists, will be clearly delineated by a positive leukocyte scan that will persist in serial imaging beyond 24 hours.

Combination imaging is helpful when a chronic nonhealing diabetic ulceration exists with or without concomitant neuropathic joint destruction. Here it is vital to identify whether an underlying infection is present, as a wound will not heal over infected soft tissue or bone. In these cases, it is most important

to discriminate between an infected ulceration and an underlying osteomyelitis (Fig. 3.11A–E) (14,48,63,65).

When performing a radionuclide leukocyte scan in the face of ulceration, it is important to note extravasations of wound exudates into dressing materials containing isotope-labeled leukocytes. This distorts the area of interest, as the radioactivity present in wound drainage can amplify the degree of uptake seen in the region of interest. Avoidance of this technical error can be accomplished by having the patient perform a dressing change immediately prior to imaging. This minimizes the accumulation of radionuclide within dressing materials and avoids misinterpretation of the image data. The negative impact that a draining ulcer has on such imaging has been documented and previously reported in the literature (63). In the case of septic joint, serial NMI should be completed at approximately 2 weeks after the completion of antibiotic therapy, as this will confirm the absence of residual infectious activity. A bone scan performed after treatment of a septic joint becomes negative as there is no residual bone remodeling or hyperemia as opposed to that seen after treatment for bone infection (Fig. 3.2A–D). After treatment for osteomyelitis, bone remodeling and hyperemia can seen on a bone scan for >1 year in many cases. Therefore, a negative ^{99m}Tc-MDP scan after treatment of a septic joint rules out the presence of an indolent inflammatory process, providing a sound basis for prognostication of the patient's outcome.

Technical errors in performing radionuclide leukocyte labeling procedures may occur at every step of the process; therefore, it is important to understand the methods and statistical strategies involved in such work. In general, a radiolabeled leukocyte compound is considered viable for use when a 90% tag or greater is confirmed by the nuclear pharmacy. This is then logged on the patient's prescription for the isotope. An insufficient label is apt to provide a poor quality exam, as the target-to-background ratio is severely hindered by an increased background radiation or low percentage label. This increase in background radiation is because of the large amount of unbound isotope circulating free within the vascular compartment. When a negative study is encountered, it is prudent to check the prescription log to ensure that the test was performed properly, that is, >90% labeling efficiency of isotopes and leukocytes for imaging. Another source of error in imaging is infiltration of the isotope at the sight of injection (Fig. 3.12). Because extremely small concentrations of isotope are used, even a partial infiltration of an injected dose will compromise the data set, as such imaging of the injection sight can be performed to rule out false-negative studies.

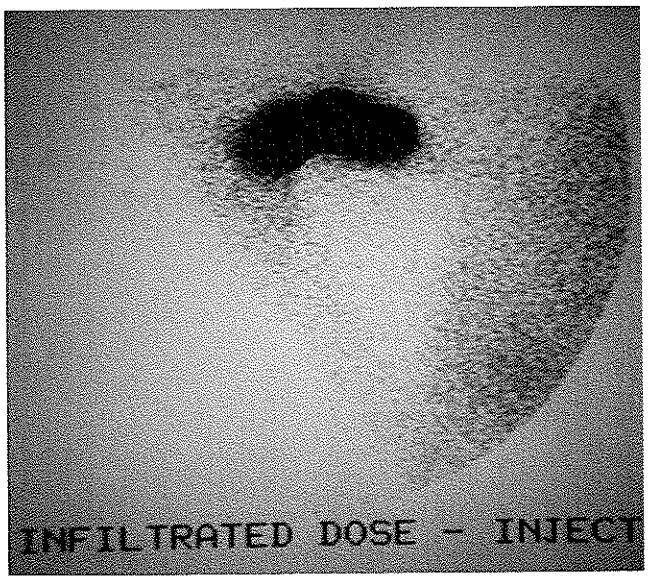

Figure 3.12 Since extremely small concentrations of isotope are used in NMI, even a partial infiltration of an injected dose will compromise the data set. As such, imaging of the injection site should be performed routinely. Here you can see the silhouette of the rib cage area and the right ante cubital area with significant infiltration of the radionuclide dose. Negative studies should always be scrutinized to rule out such technical errors before interpretation is rendered.

DIFFERENTIATION OF INFECTED VERSUS NONINFECTED NEUROPATHIC (CHARCOT) JOINT DESTRUCTION

Newman discussed six different noninfective bone and joint conditions that occur in the neuropathic foot of diabetic patients (66). Among the 67 patients reviewed in that study 6 conditions were identified listed here in a descending order of incidence: osteoarthropathy, bone loss, new bone formation, osteoporosis, spontaneous subluxations, and dislocations and pathologic fracture. Of these noninfective conditions, only pathologic fracture would be considered as a possible source of a false-positive on a radiolabeled leukocyte study. That is to say that most noninfectious conditions of the neuropathic foot in patients with diabetes should remain silent (without localized area of uptake) on NMI studies. The hallmark in treatment for these conditions is early identification and stabilization of the affected part; consequently, reliable imaging techniques become a staple in proactive therapies.

Important clinical challenges arise when faced with conditions involving actively progressive neuroarthropathy, the presence of open ulceration and clinical signs of infection in the extremity (calor, edema, erythema with or without pain). Negotiating this "Charcot triad" is perhaps the most daunting of clinical challenges. In the absence of ulceration, the differential diagnosis often includes deep vein thrombosis, cellulitis, gout, active neuroarthropathy, or deep space abscess. When ulceration is present, the suspicion for osteomyelitis or deep space abscess increases. Without frank evidence of abscess formation even MRI is unable to discern between the destruction of progressive neuroarthropathy and osteomyelitis. In some patients, there is history of previous ulceration, infection, surgery, or trauma that may confound the interpretation of some nuclear medicine imaging scans (Fig. 3.13A-C). This clinical scenario merits special attention and becomes a matter of limb salvage in populations that suffer from neuroarthropathy. With the incidence of diabetes at epidemic proportions across the country, the clinical combination of peripheral neuropathy and diabetes is on the rise, further underlining the importance of the Charcot foot in management of patients with diabetes.

Combination imaging with the benefit of ^{111}In-leukocytes and ^{99m}Tc-MDP is often helpful in distinguishing between infection and other noninfectious etiologies. Using indium as an imaging agent, it is important to understand noninfectious reasons for its uptake to ensure an accurate interpretation of the imag-

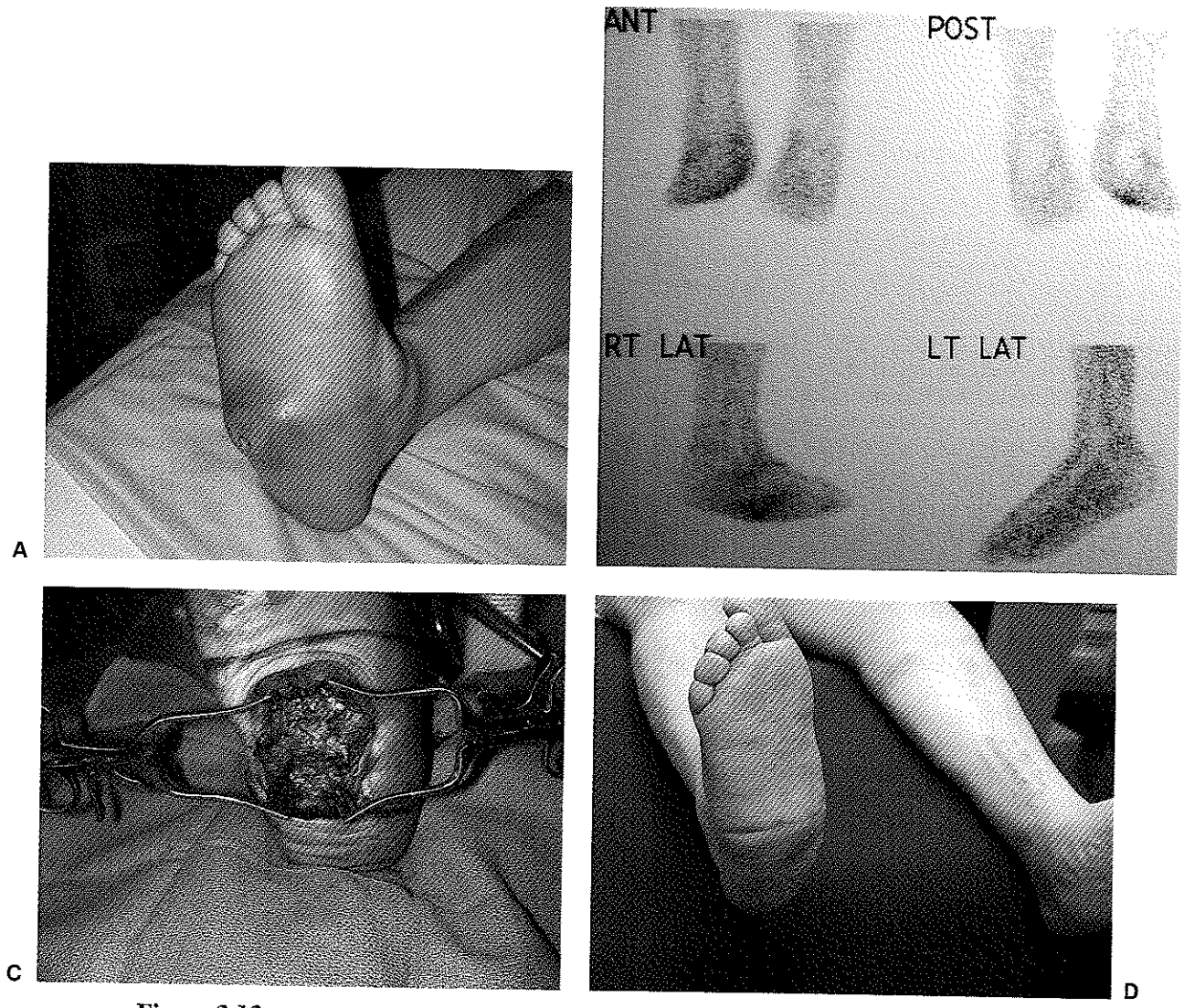

Figure 3.13 **A.** Patient with a burned out Charcot process in a clinically stable rocker bottom foot free of ulceration for 3 years. The patient presents after a 1-month history of increasing swelling, warmth, and tenderness in the right foot. Systemic signs of infection preclude imaging delays and surgical intervention is pursued emergently. **B.** This indium scan reveals the superficial nature of a localized abscess. Notice that multiple orthogonal views are required to illustrate the superficial location of this infection in the plantar midfoot. **C.** Surgical intervention for deep incision and drainage in the patient presenting with signs of foot abscess and septicemia. Necrotic and degenerative changes to the soft tissue structures of the sole are extensive and permeate two layers of the sole of the foot, seen here after irrigation. The aberrant morphology of the soft tissues and bone structures of the Charcot foot further complicate identification of local anatomic structures. Given the complex nature of the sole of the foot, this intraoperative photo illustrates why it is difficult to obtain infection imaging that can discriminate between infectious changes of soft tissue and/or bone. **D.** Limb salvage is achieved with surgical débridement, complete offloading and custom-molded ankle foot orthosis for long-term therapy. Just 1 month after surgery the entire sole is healed and ready for slow advancement to weight bearing in protective gear. Follow-up NMI was performed to confirm the absence of infection prior to releasing the patient for routine follow-up.

ing set. Table 3.2 lists some of the more common noninfectious conditions that may produce an increased uptake of isotope in an indium scan. In light of the rate of white blood cell migration in the presence of an acute infection, it seems intuitive that any radiolabeled leukocyte agent would rapidly accumulate there. In the case of the diabetic with a foot infection, one must consider that the patient's baseline hematology profile may include neutropenia, thereby reducing the potential to mount an intense leukocyte response. In fact, in many cases, the foot infection is longstanding and leukocyte margination in that event is predictably slower. This slower cellular response is a chronic process involving monocytes and mast cells rather than acute phase reactants. This is the primary reason that indium is preferred in cases of chronic infection as the use of any ^{99m}Tc compound (Tc-WBC, Tc-monoclonal antibody, or Tc-sulfur colloid) is limited by its short half-life (Table 3.1). Indium is available to be imaged

TABLE 3.2

Noninfectious Reasons for Uptake of Indium-Leukocytes

Neuroarthropathy
Heterotopic bone formation
Acute fracture <2 months
Acute bone infarct
Myositis
Active rheumatoid arthritis
Lymphoma
Post-traumatic osteoarthropathy

for a longer period of time given its protracted physical half-life (2.8 days). To further complicate the picture, from a clinical perspective, it is all too common for a patient with a Charcot joint to present months after the inciting event. Longstanding or burned out neuroarthropathy often yields deformity that is less flexible or even rigid. These cases are more prone to the development of a rocker bottom foot deformity with plantar prominences at high risk for ulceration. Plain radiographs often exhibit profound fractures and dislocations in otherwise sclerotic bone. If neuroarthropathy, acute fracture, and post-traumatic osteoarthropathy can produce a false-positive in an indium-labeled-leukocyte study, what is the value of combination imaging in these complex cases? In 1990, Seabold suggested that this clinical quandary may not be reconcilable using the combination NMI technique or even MRI. Of the 14 cases retrospectively reviewed, two Charcot patients demonstrated true-positive indium leukocyte exams, confirming osteomyelitis. Interestingly, there was no evidence of accumulation in their contralateral limbs despite the presence of chronic Charcot joint destruction. This is an important finding as it confirms that a burned out Charcot joint, despite the presence of what looks like post-traumatic osteoarthritis, does not necessarily accumulate In-WBCs (7,11). This phenomenon is demonstrated in Figure 3.7B,E in which we see a patient who has had a fifth digit amputation and biopsy of the fifth metatarsal head in addition to a chronic, burned out Charcot joint. Despite the active soft tissue and bone inflammation resulting from postsurgical change, the In-WBC scan remains negative. In 1988 and most recently in 1997, Schauwecker published his findings based on his experience as a nuclear medicine radiologist. These articles discuss the use of combination imaging of ^{99m}Tc-MDP and ^{111}In-WBC scanning in neuroarthropathy. These articles discuss findings in select cases as he describes leukocyte margination in active Charcot joint disease with a delayed washout. This phenomenon was seen in the 4-hour indium scan in which a generalized area of increased uptake was identified in the area of neuropathic destruction followed by a washout of that activity occurring by the 24-hour scan (58). This documented the leukocyte activity that takes place in the face of active, noninfectious neuroarthropathy. Consequently, the current procedure guidelines for NMI using the combination of In-WBC and ^{99m}Tc-MDP scanning suggest imaging at two intervals. Depending on the pathology to be studied, indium-WBC images should be obtained at 4 hours and again at 16 to 30 hours after injection (13). The washout phenomenon seen in the presence of a recent neuropathic fracture in an early stage of Charcot foot is demonstrated in Figure 3.10A,B. This is very different from what we see in the case of Charcot foot with an active infection and ulceration (Fig. 3.8A–D). There are two reasons that the indium-WBC imaging technique performs well in the foot. First, there are more bones in the foot than soft tissue. This means there is less background uptake of indium obscuring the region of interest, that is, the bone to soft tissue ratio is very high. Second, there is no active bone marrow in the appendicular skeleton; therefore, leukocytes do not normally accumulate there. That is to say the test has an increased sensitivity in the extremities as compared with the axial skeleton, which has active bone marrow (7). What is of particular value is being able to identify the zone of transition between an infection front and the benign inflammatory change that precedes an active infection as it migrates in tissue or bone. Nuclear medicine techniques take this challenge head-on and are able to identify the extent of inflammation that represents infection better than any other imaging technique available. This is particularly important when studying pathologic changes associated with a Charcot foot complicated by infection. The NMI scan can also be used as an anatomic guide for biopsy planning. Ultimately, the diagnosis of osteomyelitis should be confirmed by bone biopsy for adequate identification of the offending organism and determination of antibiotic sensitivity.

From a clinical perspective, combination imaging techniques using the technetium/indium protocols are routinely available; however, their use is often discouraged in favor of ^{99m}Tc-hexamethylene propylene amine oxime (HMPAO, Ceretec) imaging. This recommendation is often made blindly by technologists and radiologists for two reasons. First, because Tc-HMPAO imaging is a same-day imaging modality, it is the favored technique, requiring only a single set of images at a fixed interval after injection depending on the facility's preferred protocol. Second, imaging with a Technetium compound allows use of a general all purpose collimator in contrast to Indium that requires a high energy collimator which requires extra time and effort on the part of the technologist to prepare for. Unfortunately, the Tc-HMPAO study has a much lower target-to-background ratio than indium, and as such the resolution suffers when using the technetium agent. In fact, in the small bones of the foot Tc-HMPAO scan can result in a false-negative purely because of this imaging characteristic. In some cases of acute infection, it is reasonable to choose this agent despite the lower resolution in favor of a more expeditious surgical intervention. Certainly, this is perhaps the most important decision when dealing with a diabetic foot infection. In some instances, if surgical intervention must be performed, obtain the MRI study as soon as possible (28,67–69). This must be done with the understanding that surgical intervention will always be considered a confounding factor in interpreting any ancillary imaging technique performed after the fact. This is an important mistake that is often made when it seems easier to take a look in surgery than to completely document the location and extent of the infectious process in advance. It is not unusual to see a clinical infection evident in the heel that later develops into a process that involves the intrinsic musculature of the foot or even the Achilles tendon (Fig. 3.14A–E).

The differential diagnosis of infection in association with a complicated past medical history is an important clinical challenge commonly encountered by physicians and surgeons specializing in the lower extremity. Often, recurrent infection presents after treatment for cellulitis with ulceration, amputa-

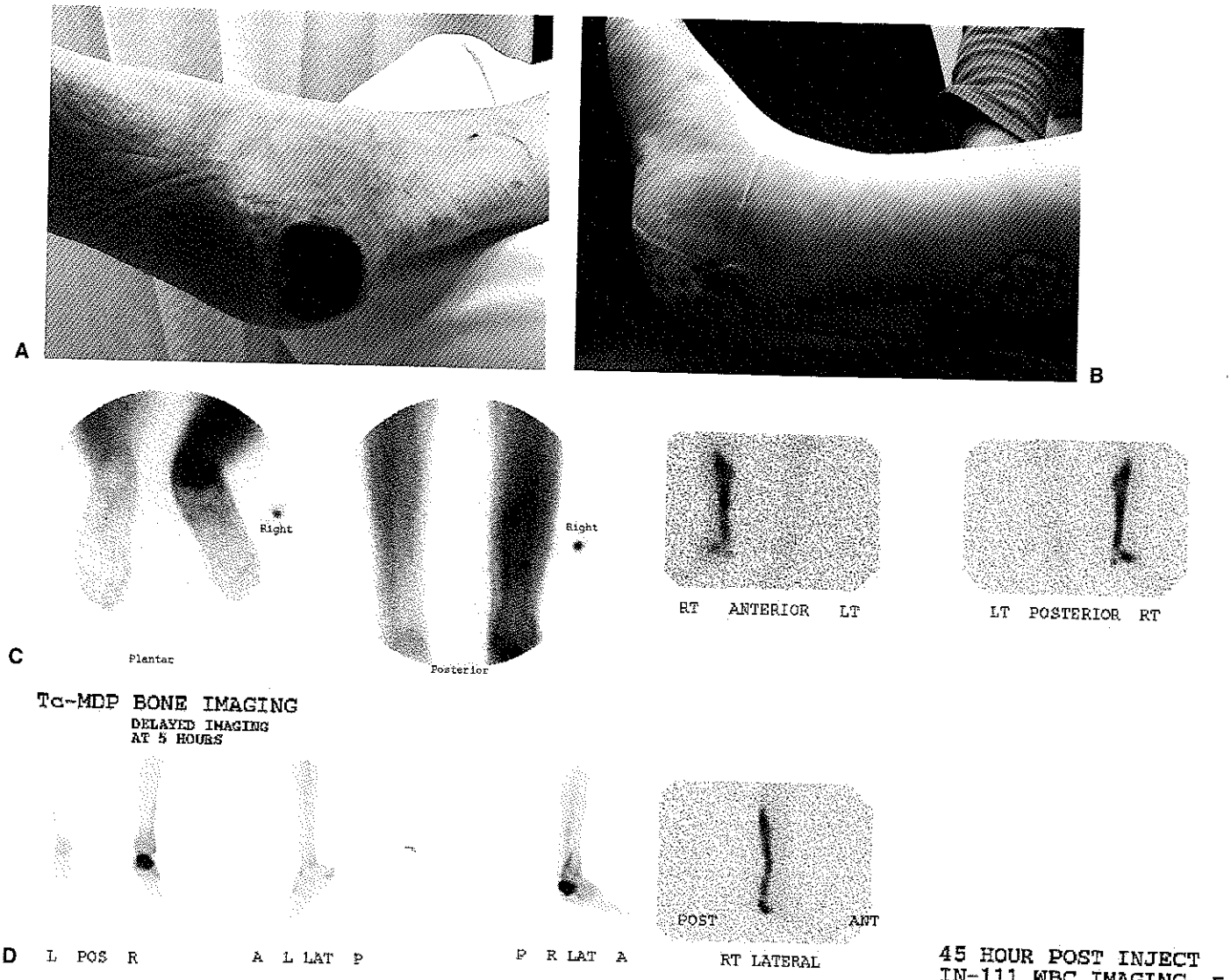

Figure 3.14 **A.** Clinical photo of posterior right heel decubitus with stable appearing eschar while under the management of a wound care center where ancillary imaging was refused in favor of local care. **B.** Clinical appearance after surgical débridement and 1 month of negative pressure therapy. **C.** ^{99m}Tc-MDP blood pool images reveal increased uptake in the plantar heel consistent with the ulceration present. Notice the outline of the vascular tree of the calf as anticipated in the second phase venous blood pool study. **D.** ^{99m}Tc-MDP third phase scan identifies a large well-localized centroid of uptake within the entire calcaneal body. **E.** Indium-labeled-leukocyte study reveals accumulation within the calcaneus as well as up the length of the Achilles tendon extending beyond the myotendinous junction. Mild erythema within the distal one third of the leg was previously suspected to be cellulitis associated with calcaneal osteomyelitis. This underlines the value of combination NMI techniques, as the Tc-MDP study alone failed to elucidate the gravity of this condition. Ultimately, limb salvage failed despite the team approach (e.g., internal medicine, infectious disease, vascular surgery, and nephrology) and ultimately an above-knee amputation was required.

tion, or other bone and joint disease in the face of chronic illness. Plain radiography often shows soft tissue edema without significant evidence of infection until 50% to 75% of the bone mineral density is lost (70). The earliest definitive signs of infection take approximately 7 to 10 days to manifest (71). Although the concept of a stage 0 neuroarthropathy has been described as the harbinger for fractures and dislocations, only increased soft tissue density on x-ray has been correlated with the clinical manifestation of the process (72). The time for such changes to develop on plain radiographs remains undetermined. Commonly, leukocyte counts, erythrocyte sedimentation rate, and blood cultures are of little value in these cases (71). As stated, the current literature clearly illustrates that NMI is clinically useful in identifying and differentiating infections of soft tissue and bone. Through clinical practice, it has been found that NMI is helpful in delineating or differentiat-

ing conditions that mimic bone infection, such as septic arthritis, gout, rheumatoid arthritis, certain bone tumors, psoriatic arthritis, and Charcot neuroarthropathy.

NMI has many clinical applications as in the case of vascular disease complicated by the presence of infection. A routine bone scan may reveal only trace or mild hyperemia in this scenario given a reduced perfusion. This is a finding that may be misinterpreted and more importantly undertreated if in fact bone is infected. Another scenario exists when a positive NMI study represents a soft tissue infection (Fig. 3.9A–C) without coincident bone infection. Here, a negative third phase ^{99m}Tc-MDP bone scan can be associated with a positive ^{111}In-oxine-WBC scan, a manifestation of infection in a calcaneal decubitus in the face of severe peripheral vascular disease. In this case, the indium study isolates soft tissue infection and by combination imaging rules out osteomyelitis. Without the benefit of the structural information provided by the ^{99m}Tc-MDP bone scan, the positivity of the indium study could easily be misinterpreted as osteomyelitis. Combination imaging in multiple orthogonal planes mapped out the region for bone biopsy and was negative for infection from both a microbiological and histologic standpoint.

The interpretation of NMI studies is chiefly the responsibility of the radiologist; however, the ordering physician should have a good working knowledge of the goals of the study and how images are to be interpreted and clinically correlated. This should include a thorough understanding of conditions that are associated with an increased leukocyte accumulation and those that are not. With this understanding, the clinician can better predict when a false-positive or -negative result is possible. This allows better prognostication for the patient and an improved clinical approach to the pathology.

Systemic diseases often manifest with pathology in the lower extremity. Complicated medical conditions such as diabetes, chronic renal failure, coronary artery disease, peripheral vascular disease, and others are compounded by the threat of infection and are among the most challenging clinical scenarios. When these perplexing cases present, there should be a meeting of minds among the surgical specialist, infectious disease specialists, radiologists, and general practitioners as to an appropriate method for obtaining a definitive diagnosis. In general, we safeguard patients by focusing on ruling out the diagnosis that carries with it the highest risk of morbidity. The consensus is that infection of soft tissue and bone carries a high degree of morbidity and merits prompt identification and treatment. In the event that infection is ruled out, the differential diagnosis can be modified and the differential list prioritized based on the clinical severity. When NMI studies are negative and serologic values remain at or return to normal, an uneventful clinical recovery is anticipated.

An obvious weakness in protocols requiring radioisotope labeling of WBCs presents in the face of patients who suffer from generalized neutropenia. Neutropenia directly impacts the total number of cells available for labeling and as such this condition diminishes the overall quality of the exam in a proportion that is consistent with the degree of neutropenia. This physiologic manifestation occurs in various disease states, including diabetes. Antibiotic therapy can be initiated immediately before imaging in these cases without affecting leukocyte labeling or interfering with imaging leukocyte accumulation. However, long-term antibiotic management prior to imaging may compromise the quality and interpretation of the NMI imaging set.

IN VIVO RADIOLABELED INFECTION IMAGING AGENTS

Research in nuclear medicine technology has focused on arriving at an ideal infection imaging agent for decades. The ideal infection imaging agent would use a low-energy isotope with a short half-life that would create an in vivo label to leukocytes, allowing for prompt imaging of infection. This would minimize radiation exposure to the patient, facilitate expeditious imaging decreasing technologist time and increase the number of patients that could be imaged in a given day. In short, the ideal agent would provide safe, fast, accurate, and inexpensive imaging of infection. To date this imaging agent does not exist. Developing such an agent is a difficult challenge. Monoclonal antibody imaging studies in animals has been going on for many years attempting to develop a technique that will be readily functional for human study. Although there are a number of in vivo radiolabeled compounds used for infection, imaging most of these techniques remain available for research purposes only (28,35,41,42,67–69,73–77). One such agent, a murine anti-CD 15 IgM monoclonal antibody, was labeled to ^{99m}technetium for infection imaging with successful phase II clinical trials reported in 1998. The CD 15 antigen is expressed at the surface of polymorphonuclear leukocytes (PMNs), monocytes, and eosinophils and so predictably aggregates in regions of infection. The agent was FDA approved in 2004 for use in imaging acute and chronic appendicitis, ischemic bowel, postsurgical infection, and nosocomial infection. The target-to-background ratio using this technique is similar to that seen in other infection imaging studies such as indium (Fig. 3.15A–C). The sensitivity and specificity in extremity imaging are similar between antibody imaging 91% and 69% and indium leukocyte imaging 91% and 62%. When interpreted with bone scans, the sensitivity reached 100% for both antibody and indium, whereas specificity was increased to 85% and 77%, respectively (73). Personal experience using this agent in a number of infection cases was very promising, and the technique has proved beneficial for complex cases such as the development of a Charcot ankle 6 months after treatment for a complex ankle fracture. It was noted that the neuropathic destruction fails to prompt accumulation of monoclonal antibodies known to aggregate in regions of infection. This documents the absence of infection in the ankle and confirms the presence of antibody uptake in a region of prior osteomyelitis resection (Fig. 3.16A–E). Chronic nonhealing ulceration in the face of longstanding diabetes and peripheral vascular disease remains suspicious for osteomyelitis of the posterior tuber until proved otherwise (Fig. 3.17A–C). Charcot ankle and chronic neuropathic fracture dislocation of the entire ankle and rear foot should have documentation that there is no evidence of deep bone infection prior to surgical reconstruction (Fig. 3.18A–H). Of note is that this form of NMI is very useful even in the small bones of the distal forefoot while this cannot be said of Tc-sulfur colloid. This is easily illustrated in the case of chronic soft tissue infection of a spider bite in the great toe. Ancillary imaging with the benefit of the NMI monoclonal antibody technique elucidated the presence of osteomyelitis in the hallux interphalangeal joint of the great toe (Fig. 3.19A–D). Similarly, chronic sesamoiditis complicated by longstanding ulceration

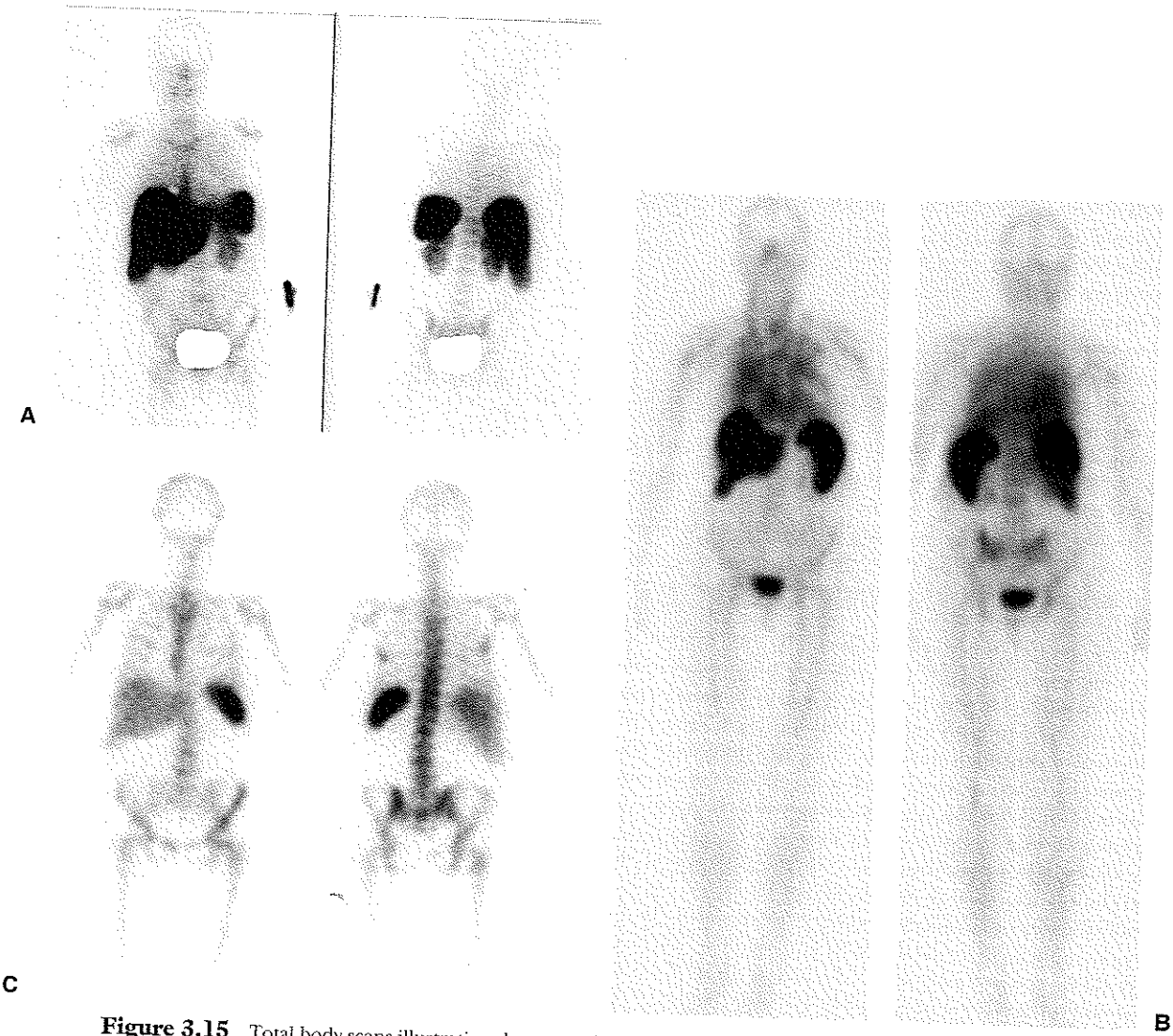

Figure 3.15 Total body scans illustrating the respective target to background ratios in normal subjects for **(A)** ^{99m}Tc-monoclonal antibody study, **(B)** ^{99m}Tc-HMPAO, and **(C)** indium leukocyte imaging.

and infection in the face of peripheral vascular disease and diabetes mellitus can be sorted out. The benefit of NMI provides distinct delineation of radiotracer uptake to confirm a well localized focus of infection despite prolonged treatment with various oral antibiotic agents and remote surgical intervention. This condition proved amenable to surgical débridement and antibiotic therapy without further bone loss (Fig. 3.20A–C). Unfortunately, because of severe adverse reactions in patients with severe underlying cardiopulmonary compromise, sales and distribution of the agent were voluntarily suspended by the end of 2005. As of the time of this printing, it is uncertain whether this agent will return for clinical applications.

PET/CT IMAGING: TECHNICAL CONSIDERATIONS IN NUCLEAR MEDICINE IMAGING OF INFECTION

Nuclear medicine imaging illuminates the distribution of radionuclide compounds by using regional, whole body, single emission computed tomography (SPECT), or positron emission tomography (PET). These techniques are all considered noninvasive, are available in area hospitals or outpatient centers, and are performed on an outpatient basis. These studies help in the diagnosis of a wide variety of pathologies beyond osteomyelitis and musculoskeletal pathology. Fungal infection, portal hypertension, appendicitis, Crohn disease, inflammatory bowel disease, and tumor imaging are but a few of the clinical conditions that NMI has been useful for over the past few decades (40–47,66–69).

Advances in nuclear medicine technology include the wide spread use of PET (72). Positron emission tomography uses a fluorine compound (F-18) labeled to the chemical fluoro-2-deoxy-d-glucose (FDG) as the basis for imaging. The energy of emission available for imaging is a 511 kV photon that is produced by the annihilation of an electron by a positron; hence, the term positron emission tomography. Original research and development of this technique focused on cerebral and cardiovascular imaging because of its ability to provide perfusion imaging. Although MRI and computed tomography (CT) are excellent tools for studying anatomic details, the PET scan is a physiologic imaging technique that reveals metabolic information about

(text continues on page 34)

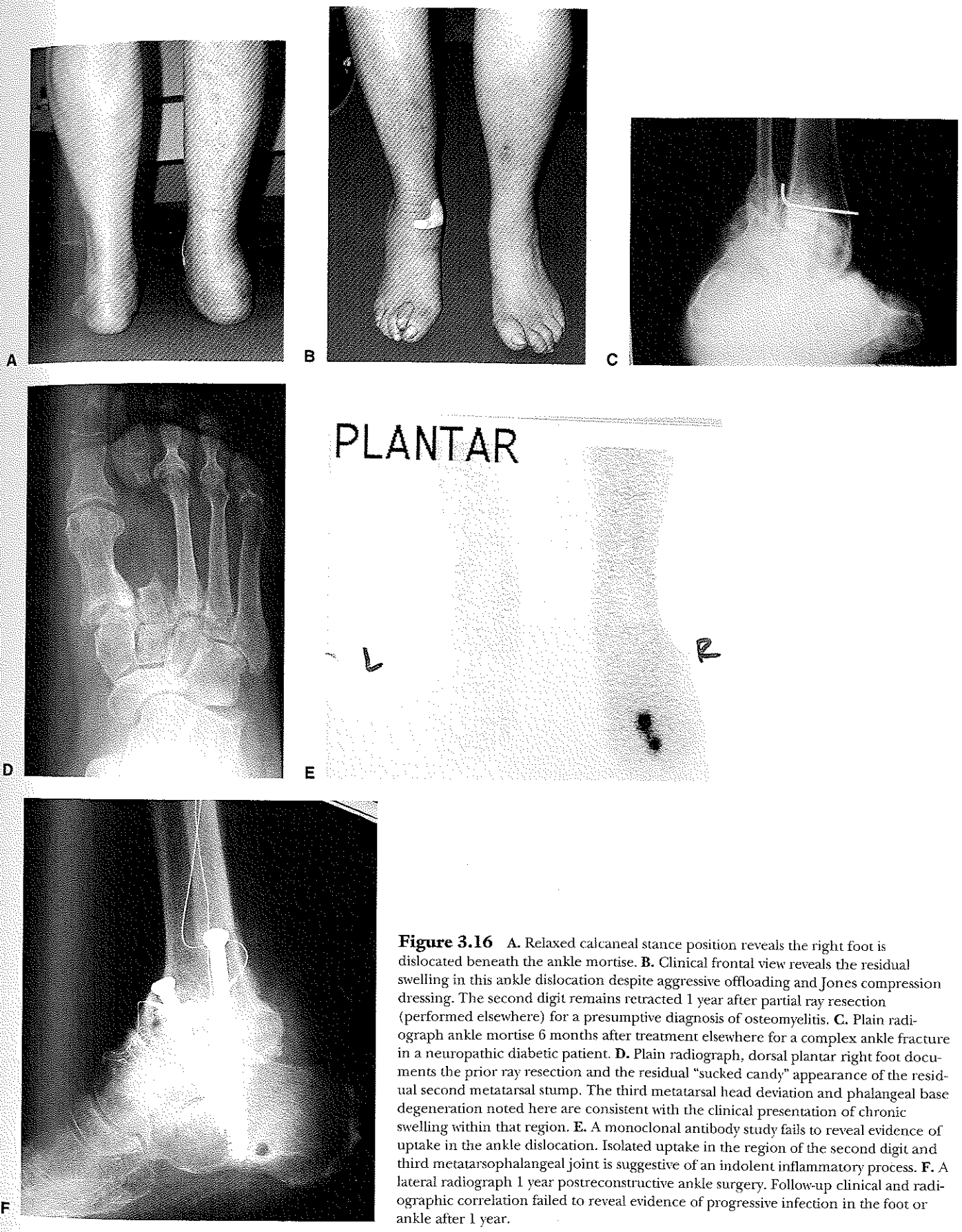

Figure 3.16 **A.** Relaxed calcaneal stance position reveals the right foot is dislocated beneath the ankle mortise. **B.** Clinical frontal view reveals the residual swelling in this ankle dislocation despite aggressive offloading and Jones compression dressing. The second digit remains retracted 1 year after partial ray resection (performed elsewhere) for a presumptive diagnosis of osteomyelitis. **C.** Plain radiograph ankle mortise 6 months after treatment elsewhere for a complex ankle fracture in a neuropathic diabetic patient. **D.** Plain radiograph, dorsal plantar right foot documents the prior ray resection and the residual "sucked candy" appearance of the residual second metatarsal stump. The third metatarsal head deviation and phalangeal base degeneration noted here are consistent with the clinical presentation of chronic swelling within that region. **E.** A monoclonal antibody study fails to reveal evidence of uptake in the ankle dislocation. Isolated uptake in the region of the second digit and third metatarsophalangeal joint is suggestive of an indolent inflammatory process. **F.** A lateral radiograph 1 year postreconstructive ankle surgery. Follow-up clinical and radiographic correlation failed to reveal evidence of progressive infection in the foot or ankle after 1 year.

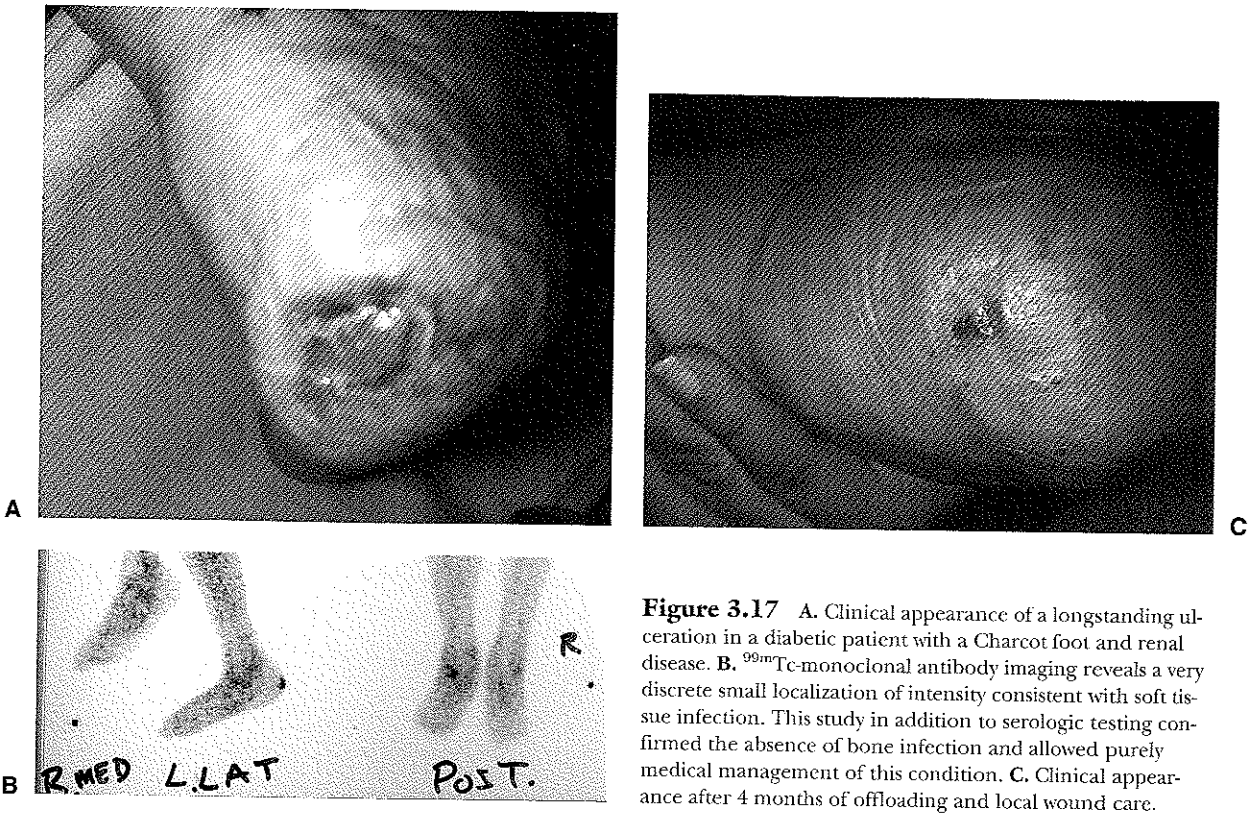

Figure 3.17 **A.** Clinical appearance of a longstanding ulceration in a diabetic patient with a Charcot foot and renal disease. **B.** ^{99m}Tc-monoclonal antibody imaging reveals a very discrete small localization of intensity consistent with soft tissue infection. This study in addition to serologic testing confirmed the absence of bone infection and allowed purely medical management of this condition. **C.** Clinical appearance after 4 months of offloading and local wound care.

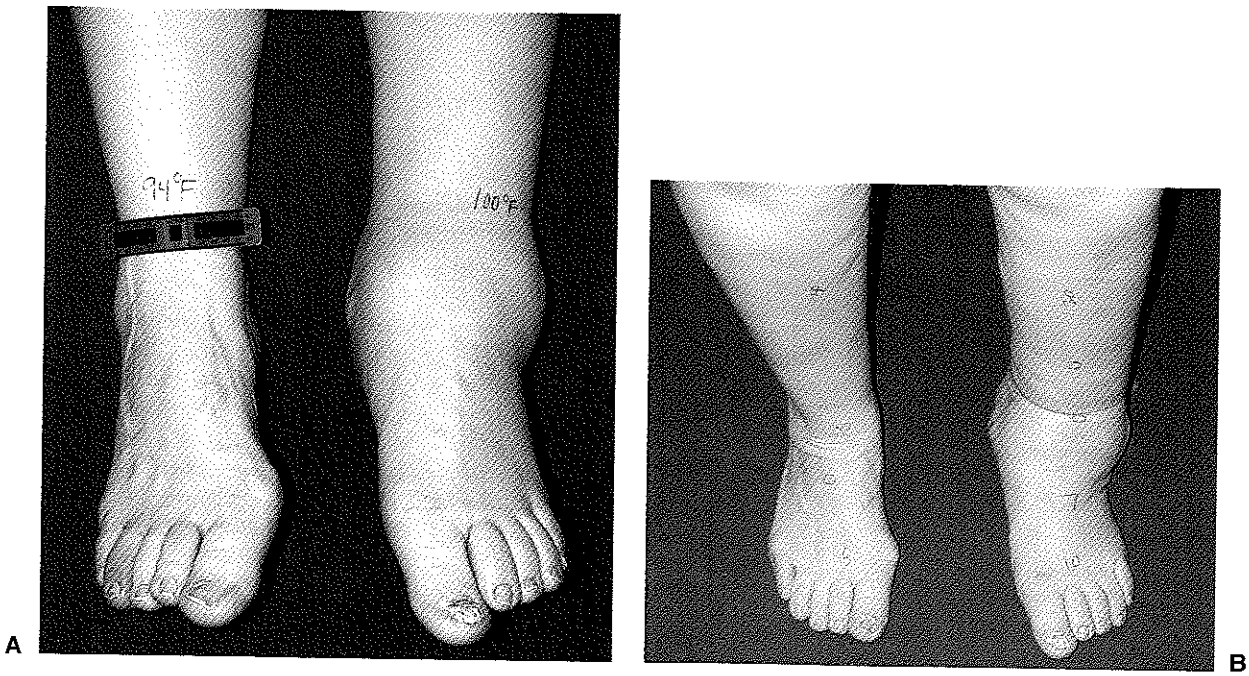

Figure 3.18 **A.** Clinical photo of left Charcot ankle dislocation demonstrating the chronic swelling and increased temperature gradient that is consistent with the Charcot process. **B.** The Charcot ankle developed subsequent to a poorly treated ankle fracture. This patient continued to walk on the limb despite the foot and ankle dislocation and extreme limb length discrepancy. *(continued)*

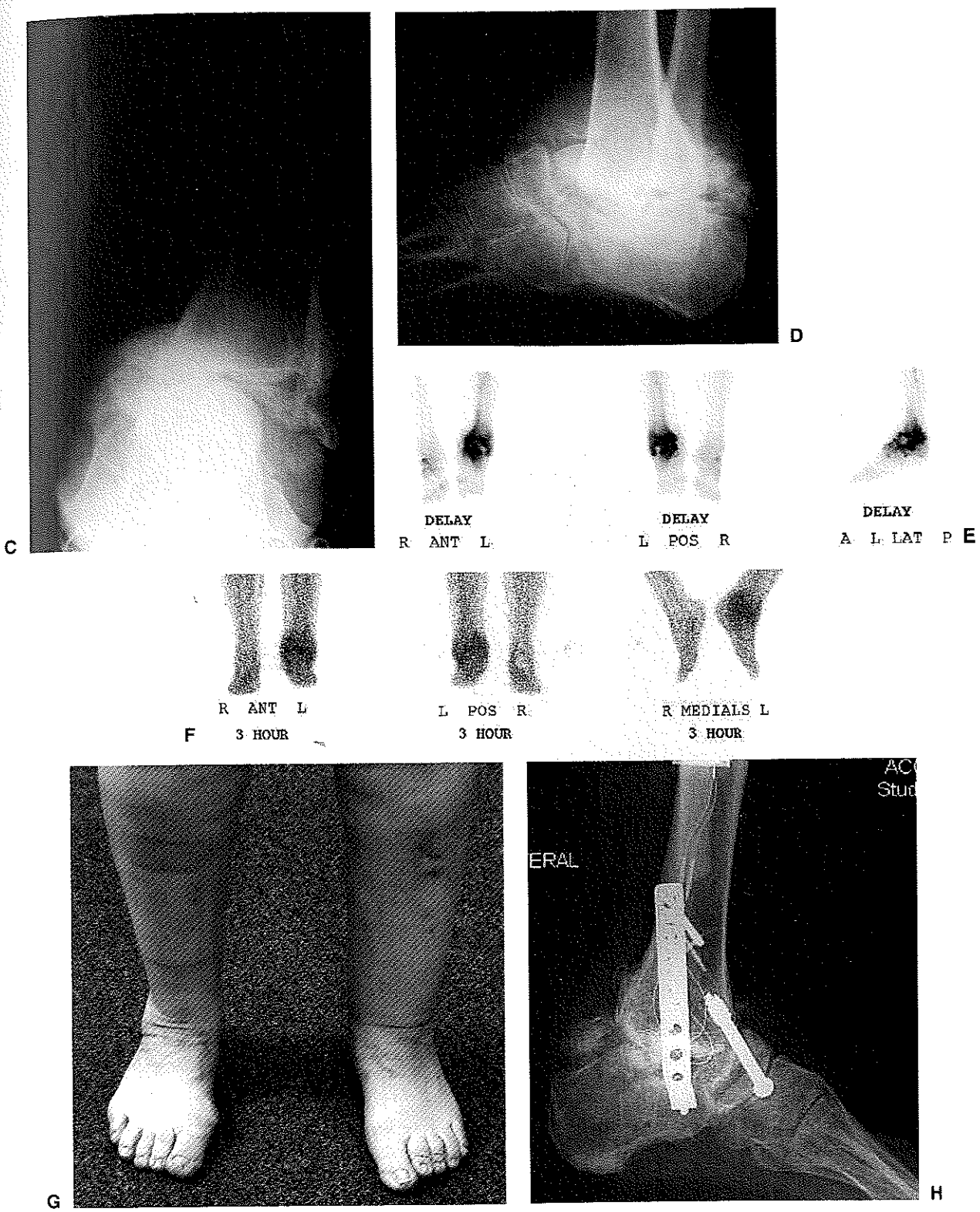

Figure 3.18 *(Continued)* **C,D.** Ankle views; anterior-posterior and lateral views revealing the dislocation and profound destruction of the Charcot process. Infection imaging is performed after detailed MRI examination fails to discriminate between the destruction of Charcot joint and osteomyelitis. **E.** ^{99m}Tc-MDP SPECT study suggests hyperemia within the bones of the ankle mortise and subtalar joint. Notice that the large ankle joint effusion makes it easier to distinguish the individual bones of the ankle mortise. **F.** ^{99m}Tc-monoclonal antibody image reveals diffuse localization within the ankle mortise. This diffuse uptake is felt to represent the florid synovial response to dead and degenerative bone fragments in and about the ankle. Subsequent bone biopsy confirms the absence of infection in the tibial plafond and the calcaneus. Both histology and microbiology were in agreement. **G.** Clinical condition 1.5 years after surgery. Surgical stabilization was pursued only after sufficient biopsy and serologic testing confirmed the absence of infection. Notice indentation markings along the right limb, indicative of prophylactic bracing. **H.** Lateral radiograph demonstrating stable consolidated tibiocalcaneal fusion, without evidence of infection 1year postoperatively.

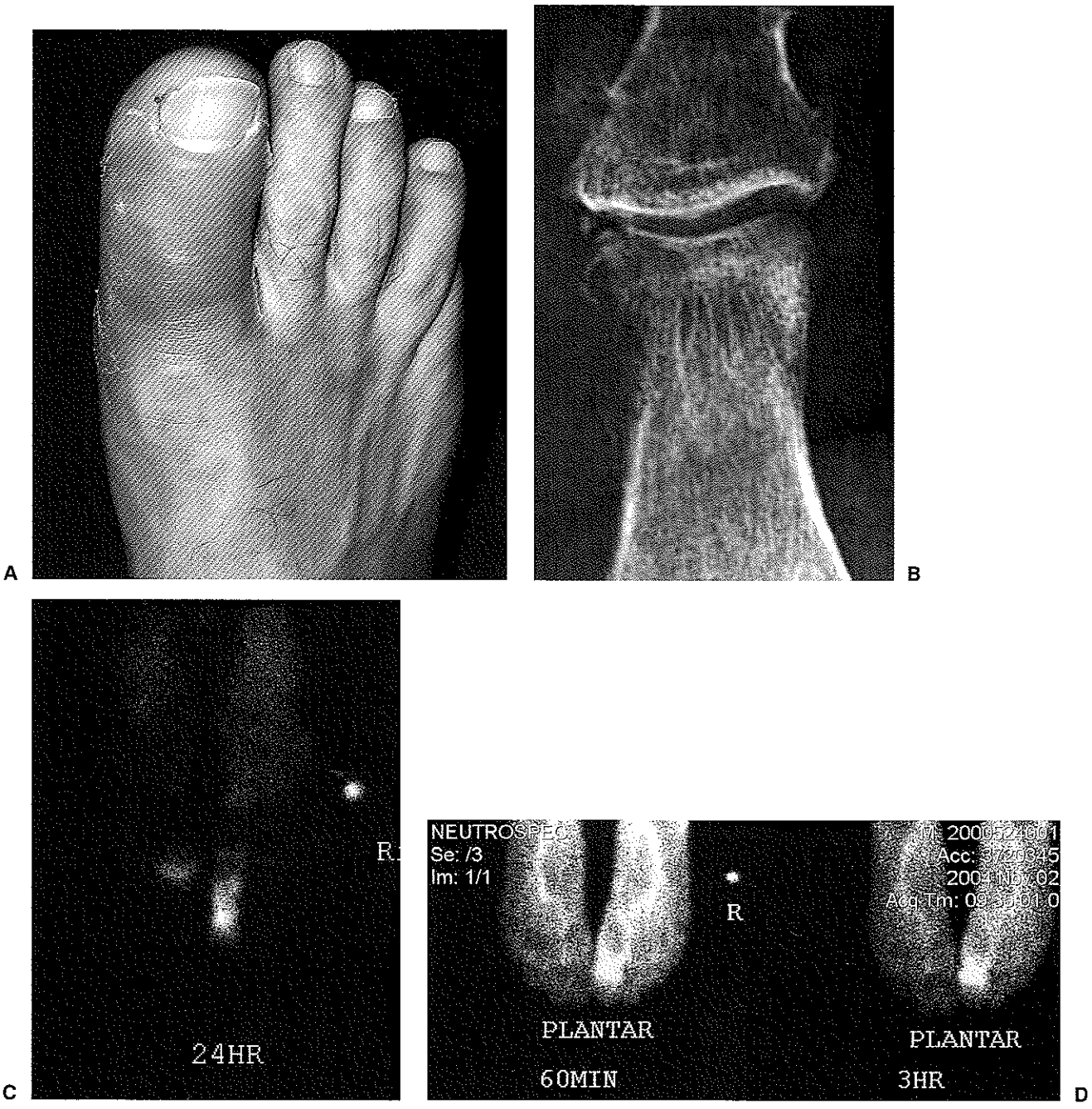

Figure 3.19 This series documents a diabetic patient who sustained a spider bite that was treated with many weeks of oral antibiotic therapy. Because of continued erythema, swelling, and pain infection imaging was pursued. **A.** Clinical evaluation reveals a tender, warm, swollen, and erythematous great toe. **B.** X-ray dorsal-plantar hallux reveals a fracture of the distal aspect of the proximal phalanx of the great toe. Arthritic changes in these regions can confound plain film interpretation and these subtle findings were overlooked upon initial presentation in the emergency room. **C.** ^{99m}Tc-MDP third phase suggests hyperemia within the hallux extending into the first metatarsal head. **D.** ^{99m}Tc-monoclonal antibody imaging performed at 60 minutes and 3 hours reveals the cubic morphology of the proximal phalanx consistent with osteomyelitis. Notice that the region of intensity found in this image set is more localized than that seen in the ^{99m}Tc-MDP scan. Partial débridement of the hallux proved curative, and indium leukocyte imaging confirmed absence of infection at long-term follow-up.

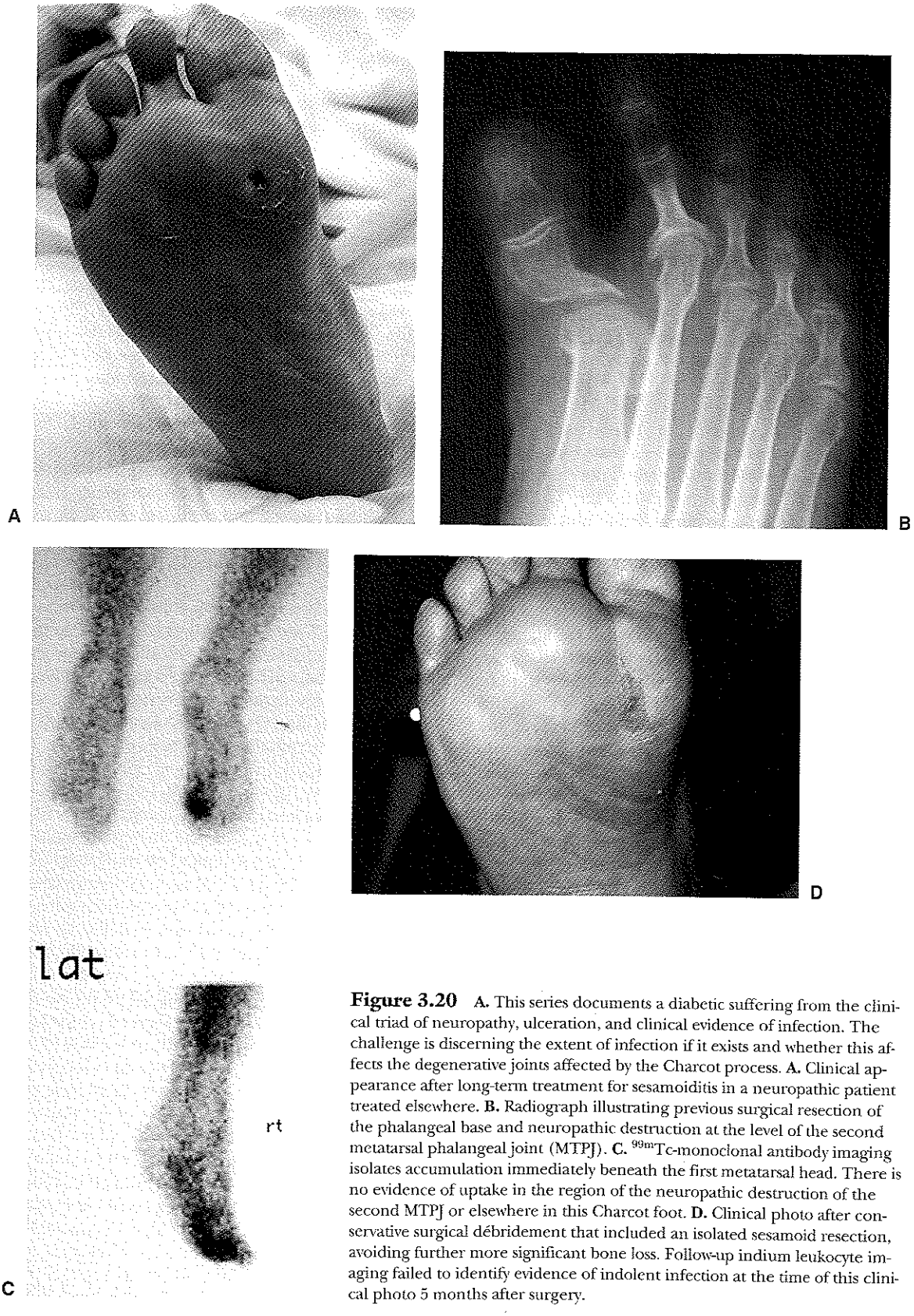

Figure 3.20 **A.** This series documents a diabetic suffering from the clinical triad of neuropathy, ulceration, and clinical evidence of infection. The challenge is discerning the extent of infection if it exists and whether this affects the degenerative joints affected by the Charcot process. **A.** Clinical appearance after long-term treatment for sesamoiditis in a neuropathic patient treated elsewhere. **B.** Radiograph illustrating previous surgical resection of the phalangeal base and neuropathic destruction at the level of the second metatarsal phalangeal joint (MTPJ). **C.** ^{99m}Tc-monoclonal antibody imaging isolates accumulation immediately beneath the first metatarsal head. There is no evidence of uptake in the region of the neuropathic destruction of the second MTPJ or elsewhere in this Charcot foot. **D.** Clinical photo after conservative surgical débridement that included an isolated sesamoid resection, avoiding further more significant bone loss. Follow-up indium leukocyte imaging failed to identify evidence of indolent infection at the time of this clinical photo 5 months after surgery.

organs before they undergo significant morphologic change. This has proved invaluable for the early identification, localization, and staging of malignancy throughout the body. This technique can be used for the follow-up of surgical resection or chemotherapy without distortion—a quality that CT and MRI do not share (78–81). In certain complex regions of interest, such as the bowel, it may be difficult to identify the anatomic location of increased radioisotope uptake of a PET scan; in these instances, the anatomic detail of a CT is required as a complement. When the metabolic information of PET is combined with the structural information of computed axial tomography, the sensitivity and specificity of this technique is markedly increased and so has moved to the forefront in diagnostic imaging. Beyer is credited with developing the first combination PET/CT scanner, which revolutionized the utility of this technique, allowing for virtually simultaneous imaging without moving the patient (82).

Malignant cells naturally have high glucose uptake, a process called facilitated transport, because of upregulated hexokinase activity. With this glucose, the tumor is able to undergo glycolysis to provide nutrients necessary for further growth. Glucose uptake is increased after the tumor has reached a threshold of 2 mm growth in diameter. This is the maximum distance that capillary permeability and diffusion can provide oxygen and nutrients for further growth. The tumor cannot grow beyond this 2-mm diameter without the upregulation of glucose to support the angiogenesis and neovascularization needed for the production of new tumor tissue. In necrotic tumors, there is an anaerobic pathway to facilitate glucose uptake for growth. Fluoro-2-deoxy-D-glucose (FDG) is an analog of glucose that is taken up by metabolically active tumor cells the same as glucose. The rate of a tumors metabolic activity is dependent upon its growth. The difference between the analog and glucose is that glucose is further broken down into by-products, whereas FDG does not. The FDG molecule becomes trapped within the metabolically active cell and remains there throughout its physiologic half-life, which allows for imaging. This metabolic imaging has many beneficial characteristics; however, anatomic resolution is not one of them. As such, additional imaging with the benefit of computed tomography is used to provide the anatomy to distinguish normal isotope uptake from the abnormal uptake of pathologic tissues.

Preparation for PET-CT imaging includes fasting for 4 to 6 hours prior to imaging, avoidance of caffeine or alcohol ingestion (although water is allowed), and abstaining from exercise activity before and after injection of the radioisotope. Immediately after injection, speaking and activity are limited to reduce muscular uptake of the FDG. The fasting is meant to enhance the FDG uptake and reduce cardiac uptake. Because FDG uptake is competitive with the patient's serum glucose, a preinjection glucose is drawn prior to injection and blood glucose of <150 mg/dL is desirable. Elevated blood glucose, reduces uptake of the radioisotope, thereby reducing the resolution of the image set. The use of insulin to reduce serum glucose during the time of imaging has been debated because insulin increases glucose transport into muscles, fat, and other tissues, and would exaggerate radioisotope uptake in these regions, potentially creating a false-positive exam. From a practical standpoint, in certain cases, it may be helpful to limit the use of regular insulin to 2 hours prior to the exam without interrupting long-acting insulin usage. The brain and liver tissues are an exception to this rule, as they do not require insulin for glucose uptake. For the CT image, 125 mL of a low-osmolarity iodine contrast medium is delivered intravenously via an injector system. Imaging is performed approximately 60 minutes after injection. The CT component of the study takes approximately 60 to 70 seconds and the PET scan approximately 30 to 45 minutes for a total body scan. The maximum patient length that can be imaged using the combination PET-CT system is 145 cm. The PET field of view is 58.8 cm with a spatial resolution of 5 mm in images processed to a thickness of 2.4 mm before fusing with the CT image. These images can be interpreted in various ways to include visual inspection, standardized uptake value (SUV), and glucose metabolism. Visual inspection of data individually from the PET and CT exam as well as fused data overlaying the two data sets is common. Standard calculations for the SUV and glucose metabolic rate have been described (83). The SUV equals trace activity in tissue (microcuries) divided by the injected radiotracer dose (millicuries)/patient body weight (kg).

Many tissues normally uptake FDG, such as the brain, heart muscle, genitourinary tract, and thymic tissue, especially in children. Sites of variable distribution include the bone marrow, gastric, and bowel tissues. Normal tissue of the liver, lung, and bone marrow range from 0.5 to 2.5 SUV, whereas malignant tumors generally have an SUV >2.5 to 3.0 (72). The liver and spleen uptake is considered low grade and diffuse; however, in the face of infection, the spleen appears hyperintense. From a practical standpoint, it is important to be consistent in timing the PET scan after injection as the isotope's half-life plays a significant role in the interpretation of the image. Similarly, it is important to grade a tumor's SUV before beginning therapy to ensure accurate interpretation of subsequent PET-CT images after therapy has been implemented.

The question remains as to whether there is a definite utility of PET-CT imaging in the diabetic foot complicated by infection, neuropathic disease, or both. Given the fundamental behavior of the radioisotope compound 18F-FDG, there may well be a place for identifying areas of increased metabolic activity of active neuropathic disease, active osteomyelitis, and other musculoskeletal indications. To date the literature is scant for PET-CT imaging in the extremities, although it is encouraged in the hunt for metastatic disease as well as follow-up of both benign and malignant neoplasm (84–87). To date, the literature using PET-CT imaging in the diabetic foot in particular is anemic and so requires much more study. Keider reported on 14 diabetic patients suspected of having foot infection (involving 18 sites). Keider used this technique and concluded that PET-CT can clarify soft tissue infection from osteomyelitis in the diabetic foot. Findings of osteomyelitis were based on histopathology and microbiology reports from biopsy specimens. Although increased uptake was seen on PET-CT imaging in both soft tissue infection and bone, this imaging set allowed exclusion of four cases that showed no abnormality, five patients with soft tissue infections only, and another site of mild intensity in osteoarthropathy associated with diabetes. Ultimately, PET-CT identified osteomyelitis in four patients localizing eight sites of infection that were confirmed by microbiology (88). Given the research that has been completed in nuclear medicine infection imaging it is intuitive that the nature of an infection exhibited in NMI scanning is more closely related to the cellular activity of the affected tissue than whether the condition is acute or chronic in nature. Therefore, it stands to reason that PET-CT should be affective in

identifying both acute and chronic conditions of infection while elucidating important structural information. Mochizuki et al and Paik et al suggested that the cellular uptake of FDG in the presence of inflammation and infection is ultimately because of the activity of various cytokines and growth factors that increase the number of glucose transporters and their affinity to FDG (89,90). As of the date of this writing, PET-CT imaging has moved to the forefront in three-dimensional imaging; however, to date it only has FDA approval for indications within the realm of oncology (72,78–91). Although it is understood that physicians have used this technique for off-label indications such as infection imaging, the technique remains a modality to which most clinicians have only limited access.

CONCLUSION

Nuclear medicine leukocyte imaging (NMLI) for the diagnosis of infection has been discussed and used by the medical community for decades. Although these studies have withstood the test of time, this imaging technique has a specificity that is less than desirable. The use of combination imaging, ^{111}indium or ^{99m}technetium leukocyte images in combination with a ^{99m}TC-MDP bone scan, can afford greater anatomic information and elucidate discrete areas of infection, thereby increasing the specificity of NMI.

The use of nuclear medicine imaging for infection and combination imaging techniques (^{111}In-WBC and ^{99m}Tc-WBC/^{9m}Tc-MDP) has tremendous utility for the surgical physician, as it not only identifies the presence of disease but also provides a mechanism for monitoring therapy and ultimately confirming when the disease has been successfully eradicated. This has been demonstrated and discussed in the current literature extensively (2–38,48,49,52–63,65,92–94). Specifically, the leukocyte imaging technique can be repeated weeks or months after treatment, confirming the eradication of infection. Most importantly, in cases of immunocompromise and history of exacerbations and remissions of infection these studies can rule out the presence of indolent infection residual of prior therapy. This allows for better prognostication in patient management and prevents insufficient treatment of infection and recurrence. In addition, serial imaging techniques can be employed in a manner that can help minimize or reduce the duration of antibiotic therapy. This reduces morbidity secondary to the renal toxicity that many antibiotics impose.

Further work in nuclear medicine technology should include improving strategies to delineate regions of interest within the small bones of the foot. This may be possible using combination NMI with tomography and digital subtraction protocols for isolation of individual bones within the tarsus and lesser tarsal bones.

Perhaps the greatest strength in nuclear medicine imaging for the lower extremity is its ability to identify and isolate infectious processes, differentiating them from other more benign clinical conditions.

ACKNOWLEDGMENTS

Thanks are due to the medical library staff of Mercy Health Partners, with special thanks to all of those working at St. Vincent Mercy Medical Center, Toledo, OH. Thanks, too, to the nuclear medicine technologists at Mercy Health Partners of Toledo, OH, and St. Luke's Hospital, Maumee, OH, with special thanks to those at St. Vincent Mercy Medical Center, Toledo, OH.

REFERENCES

1. Seldin DW, Heiken JP, Feldman F, et al. Effect of soft-tissue pathology on detection of pedal osteomyelitis in diabetics. J Nucl Med 1985;26:988–993.
2. Alazraki NP. Gallium-67 imaging in infection. In: Early PJ, Sodee DB, eds. Principles and practice of nuclear medicine. 2nd ed. St. Louis: Mosby; 1995: 702–713.
3. Thakur ML, Coleman RE, Mayhall CG, et al. Preparation and evaluation of ^{111}In-labeled leukocytes as an abscess imaging agent in dogs. Radiology 1976;119:731.
4. Preston DF. Indium-111 label in inflammation and neoplasm imaging. In: Early PJ, Sodee DB, eds. Principles and practice of nuclear medicine. 2nd ed. St. Louis: Mosby; 1995:714–724.
5. McAfee JG, Thakur ML. Survey of radioactive agents for in vitro labeling of phagocytic leukocytes. 1. Soluble agent. J Nucl Med 1976;17:480–487.
6. McAfee JG, Thakur ML. Survey of radioactive agents for in vitro labeling of phagocytic leukocytes. 2. Particles. J Nucl Med 1976;17:488–492.
7. Schauwecker DS, Park HM, Burt RW, et al. Combined bone scintigraphy and indium-111 leukocyte scans in neurotrophic foot disease. J Nucl Med 1988; 29(10):1651–1655.
8. Datz FL, Thorne DA. Effect of chronicity of infection on the sensitivity of the In-111-labeled leukocyte scan. Am J Roentgenol 1986;147:809–812.
9. Keenan AM, Tindel NL, Alavi A. Diagnosis of pedal osteomyelitis in diabetic patients using current scintigraphic techniques. Arch Intern Med 1989;149: 2262–2266.
10. Nepola JV, Seabold JE, Marsh JL, et al. Diagnosis of infection in ununited fractures. J Bone Joint Surg Am 1993;75(12):1816–1822.
11. Seabold JE, Flickinger FW, Kao SC, et al. Indium-111-leukocyte/technetium-99m-MDP bone and magnetic imaging: difficulty in diagnosing osteomyelitis in patients with neuropathic osteoarthropathy. J Nucl Med 1990;31:549–556.
12. Palestro CJ, Kim CK, Swyer AJ, et al. Total-hip arthroplasty: periprosthetic indium-111-labeled leukocyte activity and complementary technetium-99m-sulfur colloid imaging in suspected infection. J Nucl Med 1990;31(12): 1950–1955.
13. Seabold JE, Forstrom LA, Schauwecker DS, et al. Procedure guideline for indium-111-leukocyte scintigraphy for suspected infection/inflammation. J Nucl Med 1997;38:997–1001.
14. Larcos G, Brown ML, Sutton RT. Diagnosis of osteomyelitis of the foot in diabetic patients: value of In-111-leukocyte scintigraphy. AJR 1991;157:527–531.
15. Palestro CJ, Mehta HH, Patel M, et al. Marrow versus infection in the Charcot joint: indium-111 leukocyte and technetium-99m sulfur colloid scintigraphy. J Nucl Med 1998;39(2):346–350.
16. Magnuson JE, Brown ML, Hauser MF, et al. In-111-labeled leukocyte scintigraphy in suspected orthopedic prosthesis infection: comparison with other imaging modalities. Radiology 1988;168:235–239.
17. McAfee JG, Gagne G, Subramanian G, et al. The localization of indium-111-leukocytes, gallium-67-polyclonal IgG and other radioactive agents in acute focal inflammatory lesions. J Nucl Med 1991;32(11):2126–2131.
18. Baldwin JE, Wraight EP. Indium labeled leukocyte scintigraphy in occult infection: a comparison with ultrasound and computed tomography. Clin Radiol 1990;42:199–202.
19. Peters AM. The utility of (99mTc)HMPAO-leukocytes for imaging infection. Semin Nucl Med 1994;24(2):110–127.
20. Kao CH, Huang WT, Wang YL, et al. A comparative study of Tc-99m-HMPAO and Tc-99m-ECD as a leukocyte labelling agent. Nucl Med Commun 1994;15: 294–297.
21. Hovi I. Complicated bone and soft-tissue infections. Imaging with 0.1 T MR and 99mTc-HMPAO-labeled leukocytes. Acta Radiol 1996;37:870–876.
22. Datz FL, Seabold JE, Brown ML, et al. Procedure guideline for technetium-99m-HMPAO-labeled leukocyte scintigraphy for suspected infection/inflammation. J Nucl Med 1997;38(6):987–990.
23. Devillers A, Moisan A, Hennion F, et al. Contribution of technetium-99m hexamethylpropylene amine oxime labelled leukocyte scintigraphy to the diagnosis of diabetic foot infections. Eur J Nucl Med 1998;25(2):132–138.
24. Shih WJ, Han JK, Magoun S, et al. Detection of abscesses with Tc-99m HMPAO leukocyte scintigraphy depends on their stage and location. Clin Nucl Med 1999;24(2):111–114.

25. Roca M, Martín-Comín J, Becker W, et al. A consensus protocol for white blood cells labelling with technetium-99m hexamethylpropylene amine oxime. Eur J Nucl Med 1998;25(7):797–799.
26. Reynolds JH, Graham D, Smith FW. Imaging inflammation with Tc-99m-HMPAO labeled leucocytes. Clin Radiol 1990;42:195–198.
27. Vorne M, Soini I, Lantto T, et al. Technetium-99m HM-PAO-labeled leukocytes in detection of inflammatory lesions: comparison with gallium-67 citrate. J Nucl Med 1989;30(8):1332–1336.
28. Rüther W, Hotze A, Möller F, et al. Diagnosis of bone and joint infection by leucocyte scintigraphy. A comparative study with Tc-99m-HMPAO-labeled leucocytes, 99mTc-labelled antigranulocyte antibodies and 99mTc-labelled nanocolloid. Arch Orthop Trauma Surg 1990;110:26–32.
29. Moragas M, Lomeña F, Herranz R, et al. Tc-99m-HMPAO-leukocyte scintigraphy in the diagnosis of bone infection. Nucl Med Comm 1991;12: 417–427.
30. Lantto T, Kaukonen JP, Kokkola A, et al. Tc-99m HMPAO labeled leukocytes superior to bone scan in the detection of osteomyelitis in children. Clin Nucl Med 1992;17:7–10.
31. Bennett JD, Dubeau RA, Driedger AA, et al. Polymorphonuclear leukocytes labeled with technetium-99m HMPAO. A potential bone marrow imaging agent. Clin Nucl Med 1987;9:44–45.
32. Roddie ME, Peters AM, Danpure HJ, et al. Inflammation: imaging with Tc-99m HMPAO-labeled leukocytes. Radiology 1988;166:767–772.
33. Copping C, Dalgliesh SM, Dudley NJ, et al. The role of 99mTc-HMPAO white cell imaging in suspected orthopaedic infection. Br J Radiol 1992;65: 309–312.
34. Esper EL, Dacquet V, Paillard J, et al. 99mTc-HMPAO-labelled leukocyte scintography in suspected chronic osteomyelitis related to an orthopaedic device: clinical usefulness. Nucl Med Comm 1992;13:799–805.
35. Vorne M, Lantto T, Paakkinen S, et al. Clinical comparison of Tc-99m-HMPAO labeled leucocytes and Tc-99m-nanocolloid in the detection of inflammation. Acta Radiol 1989;30:633–637.
36. Mortelmans L, Verlooy H, Nevelsteen A, et al. Clinical usefulness of Tc-99m-HMPAO labeled white blood cell imaging in prosthetic vascular graft infections. Clin Nucl Med 1992;17:11–13.
37. Hotze A, Bockisch A, Rüther M, et al. Comparison of Tc-99m-HMPAO-labelled leukocytes and 99mTc-nanocolloid in osteomyelitis. Nucl Med 1988;27:63–65.
38. Winker H, Reuland P, Muller J, et al. Leukocyte scintography with 99mTc-HMPAO in the diagnosis of bone inflammations. Nucl Med 1988;27:121–125.
39. Prats E, Banzo J, Abós MD, et al. Diagnosis of prosthetic vascular graft infection by technetium-99m-HMPAO-labeled leukocytes. J Nucl Med 1994;35(8): 1303–1307.
40. Fox IM, Zeiger L. Tc-99m-HMPAO leukocyte scintigraphy for the diagnosis of osteomyelitis in diabetic foot infections. J Foot Ankle Surg 1993;32: 591–594.
41. Sunshine JL, Gentili A. Imaging of disseminated infection by a rare fungal pathogen, Fusarium. Clin Nucl Med 1994;19(5):435–437.
42. Manns RA, Vickers CR, Chesner IM, et al. Portal hypertension secondary to sigmoid colon arteriovenous malformation. Clin Radiol 1990; 42:203–204.
43. Laitinen R, Tahtinen J, Lantto T, et al. Tc-99m-HMPAO leukocytes in imaging of patients with suspected acute abdominal inflammation. Clin Nucl Med 1990;15:597–602.
44. Hughes JP, Rees JI, Facey P. Scintigraphic demonstration of a blind loop following surgery for Crohn's disease—the value of Tc-99m-HMPAO white cell scanning. Clin Nucl Med 1994;19:469–470.
45. Evetts BK, Foley CR, Latimer RG, et al. Tc-99 hexamethylpropyleneamineoxide scanning for the detection of acute appendicitis. J Am Coll Surg 1994;179: 197–201.
46. Bhargava SA, Orenstein SR, Charron M. Tecnetium-99m hexamethylpropyleneamine-oxime-labeled leukocyte scintigraphy in inflammatory bowel disease in children. J Pediatr 1994;125:213–217.
47. Lantto EH, Lantto TJ, Vorne M. Fast diagnosis of abdominal infections and inflammations with technetium-99m-HMPAO labeled leukocytes. J Nucl Med 1991;32(11):2029–2034.
48. Palestro CJ, Tomas MB. Scintigraphic evaluation of the diabetic foot. Nucl Med Ann 2000;143–171.
49. Vesco L, Boulahdour H, Hamissa S, et al. The value of combined radionuclide and magnetic resonance imaging in the diagnosis and conservative management of minimal or localized osteomyelitis of the foot in diabetic patients. Metabolism 1999;48(7):922–927.
50. Spaeth HJ Jr, Dardani M. Magnetic resonance imaging of the diabetic foot. Magn Reson Imaging Clin Am 1994;2(1):123–130.
51. Beltran J, McGhee RB, Shaffer PB, et al. Experimental infections of the musculoskeletal system: evaluation with MR imaging and Tc-99m MDP and Ga-67 scintigraphy. Radiology 1988;167:167–172.
52. Chandnani VP, Beltran J, Morris CS, et al. Acute experimental osteomyelitis and abscesses: detection with MR imaging versus CT. Radiology 1990; 174:233–236.
53. Unger E, Moldofsky P, Gatenby R, et al. Diagnosis of osteomyelitis by MR imaging. Am J Roentgel 1988;150:605–610.
54. Wang A, Weinstein D, Greenfield L, et al. MRI and diabetic foot infections. Magn Reson Imaging 1990;8:805–809.
55. Beltran J, Campanini DS, Knight C, et al. The diabetic foot: magnetic resonance imaging evaluation. Skeletal Radiol 1990;19:37–41.
56. Moore TE, Yuh WT, Kathol MH, et al. Abnormalities of the foot in patients with diabetes mellitus: findings on MR imaging. Am J Roentgel 1991; 157:813–816.
57. Weinstein D, Wang A, Chambers R, et al. Evaluation of magnetic resonance imaging in the diagnosis of osteomyelitis in diabetic foot infections. Foot Ankle 1993;14:18–22.
58. Schauwecker DS. Differentiation of infected from noninfected rapidly progressive neuropathic osteoarthropathy. J Nucl Med 1995;36(8):1427–1428.
59. Alazraki NP. Editorial. Diagnosing prosthetic joint infection. J Nucl Med 1990;31(12):1955–1957.
60. Palestro CJ, Torres MA. Radionuclide imaging in orthopedic infections. Semin Nucl Med 1997;27(4):334–345.
61. Elgazzar AH, Abdel-Dayem HM. Imaging skeletal infections: evolving considerations. Nucl Med Ann 1999;92:157–191.
62. Seabold JE, Nepola JV. Imaging techniques for evaluation of postoperative orthopedic infections. Q J Nucl Med 1999;43(1):21–28.
63. Palestro CJ, Cohen IR, Goldsmith SJ. Wound dressing activity mimicking infection on labeled leukocyte imaging. Clin Nucl Med 1991;17:711–713.
64. Sinha S, Munichoodappa CS, Kozak GP. Neuro-arthropathy (Charcot joints) in diabetes mellitus (clinical study of 101 cases). Medicine (Baltimore) 1972;51(3):191–210.
65. Newman LG, Waller J, Palestro CJ, et al. Unsuspected osteomyelitis in diabetic foot ulcers. JAMA 1991;266(9):1246–1251.
66. Newman JH. Non-infective disease of the diabetic foot. J Bone Joint Surg Br 1981;63-B(4): 593–596.
67. Becker W, Palestro CJ, Winship J, et al. Rapid imaging of infections with a monoclonal antibody fragment (LeukoScan). Clin Orthop Relat Res 1996; 329:263–272.
68. Goins B, Klipper R, Rudolph AS, et al. Use of technetium-99m-liposomes in tumor imaging. J Nucl Med 1994;35:1491–1498.
69. Becker W, Bair J, Behr T, et al. Detection of soft-tissue infections and osteomyelitis using a technetium-99m-labeled anti-granulocyte monoclonal fragment. J Nucl Med 1994;35(9):1436–1443.
70. Hankins CA, Braunstein EM. Osteomyelitis. Imaging modalities and diagnostic approach. Postgrad Radiol 1984;4:75.
71. Feigin DS, Strauss HW, James AE. The bone marrow scan in experimental osteomyelitis. Skel Radiol 1976;1:103–111.
72. Yu GV, Hudson JR. Evaluation and treatment of stage 0 Charcot's neuroarthropathy of the foot and ankle. J Am Podiatr Med Assoc 2002;92(4): 210–220.
73. Palestro CJ, Kipper SL, Weiland FL, et al. Osteomyelitis: diagnosis with 99mTc-Labeled antigranulocyte antibodies compared with diagnosis with Indium labeled leukocytes. Initial experience. Radiology 2002;223(3):758–764.
74. Thakur ML, Marcus CS, Henneman P, et al. Imaging inflammatory diseases with neutrophil-specific technetium-99m-labeled monoclonal antibody anti-SSEA-1. J Nucl Med 1996;37:1789–1795.
75. Mozley PD, Thankue ML, Alavi A, et al. Effects of a 99mTc-labeled murine immunoglobulin M antibody to CD15 antigens on human granulocyte membranes in healthy volunteers. J. Nucl Med 1999;40:2107–2114.
76. Gratz S, Behr T, Herrmann A, et al. Intraindividual comparison of 99mTc-labelled anti-SSEA-1 antigranulocyte antibody and 99mTc-HMPAO labelled white blood cells for the imaging of infection. Eur J Nucl Med 1998;25:386–393.
77. Kipper SL, Rypins EB, Evans DG, et al. Neutrophil-specific 99mTc-labeled anti-CD15 monoclonal antibody imaging for diagnosis of equivocal appendicitis. J Nucl Med 2000;41:449–455.
78. Eubank WB, Mankoff DA, Schmiedl UP, et al. Imaging of oncologic patients: benefit of combined CT and FDG PET in the diagnosis of malignancy. AJR Am J Roentgenol 1998;171:1103–1110.
79. Wahl RL, Quint LE, Cieslak RD, et al. Anatometabolic tumor imaging: fusion of FDG PET with CT or MRI to localize foci of increased activity. J Nucl Med 1993;34:1190–1197.

80. Pietrzyk U, Herholz K, Heiss WD. Three-dimensional alignment of functional and morphological tomograms. J Comput Assist Tomogr 1990;14: 51–59.
81. Armstrong DG, Lavery LA, Sariaya M, Ashry H. Leukocytosis is a poor indicator of Acute Osteomyelitis of the foot in diabetes mellitus. J Foot Ankle Surg 1995;35(4):280–283.
82. Beyer T, Townsend DW, Brun T, et al. A combined PET/CT scanner for clinical oncology. J Nucl Med 2000;41:1369–1379.
83. Kapoor V, McCook BM, Torok FS. An introduction to PET-CT imaging. Radiographics 2004;24(2):523–543.
84. Niederkohr R, Rosenberg J, Shabo G, et al. Clinical value of including the head and lower extremities in 18F-FDG PET/CT imaging for patients with malignant melanoma. Nucl Med Commun 2007;28(9):688–695.
85. Iagaru A, Hendersen R. PET/CT follow-up in nonossifying fibroma. AJR Am J Roentgenol 2006;187(3):830–832.
86. Goodin GS, Shulkin BL, Kaufman RA, et al. PET/CT characterization of fibroosseous defects in children: 18F-FDG uptake can mimic metastatic disease. AJR Am J Roentgenol 2006;187(4):1124–1128.
87. Schöder H, Larson SM. Positron emission tomography for prostate, bladder, and renal cancer. Semin Nucl Med 2004;34:274–292.
88. Keidar Z, Militianu D, Melamed E, et al. The diabetic foot: initial experience with 18F-FDG PET/CT. J Nucl Med 2005;46(3):444–449.
89. Mochizuki T, Tsukamoto E, Kuge Y, et al. FDG uptake and glucose transporter subtype expressions in experimental tumor and inflammation models. J Nucl Med 2001;42:1551–1555.
90. Paik JY, Lee KH, Choe YS, et al. Augmented 18F-FDG uptake in activated monocytes occurs during the priming process and involves tyrosine kinases and protein kinase C. J Nucl Med 2004;45:124–128.
91. Palestro CJ, Love C, Miller TT. Diagnostic imaging tests and microbial infections. Cell Microbiol 2007;9(10):2323–2333.
92. Palestro CJ, Love C, Tronco GG, et al. Role of radionuclide imaging in the diagnosis of postoperative infection. Radiographics 2000;20:1649–1660.
93. Demopulos GA, Bleck EE, McDougall IR. Role of radionuclide imaging in the diagnosis of acute osteomyelitis. J Pediatr Orthop 1988;8:558–565.
94. Roddie ME, Peters AM, Osman S, et al. Osteomyelitis. Nucl Med Commun 1988;9:713–717.

Surgical Reconstruction of the Diabetic Foot and Ankle

EDITOR

Thomas Zgonis, DPM, FACFAS

Associate Professor, Department of Orthopaedic Surgery
Chief, Division of Podiatric Medicine and Surgery
Director, Podiatric Surgical Residency and Fellowship Programs
The University of Texas Health Science Center at San Antonio
San Antonio, Texas

Wolters Kluwer | Lippincott Williams & Wilkins
Health

Philadelphia • Baltimore • New York • London
Buenos Aires • Hong Kong • Sydney • Tokyo

Acquisitions Editor: Robert Hurley
Product Manager: David Murphy Jr.
Production Manager: Alicia Jackson
Senior Manufacturing Manager: Benjamin Rivera
Marketing Manager: Lisa Parry
Design Coordinator: Teresa Mallon
Production Services: Maryland Composition/ASI

530 Walnut Street
Philadelphia, PA 19106 USA
LWW.com

Printed in the People's Republic of China

Library of Congress Cataloging-in-Publication Data

ISBN 978-0-7817-8458-0

Surgical reconstruction of the diabetic foot and ankle / Thomas Zgonis.—1st ed.
p. ; cm.
Includes bibliographical references and index.
1. Foot—Surgery. 2. Ankle—Surgery. 3. Diabetes—Surgery. I. Zgonis, Thomas.
[DNLM: 1. Diabetic Foot—surgery. 2. Limb Salvage. 3. Reconstructive Surgical Procedures—methods. WK 835 S9615 2010]
RD563.S88 2010
617.5'85059—dc22

2009003111

To purchase additional copies of this book, call our customer service department at (800) 638-3030 or fax orders to (301) 223-2320. International customers should call (301) 223-2300.

Visit Lippincott Williams & Wilkins on the Internet: at LWW.com. Lippincott Williams & Wilkins customer service representatives are available from 8:30 am to 6 pm, EST.

10 9 8 7 6 5 4 3 2 1

CCS0509